JCI The Journal of Clinical Investigation

Prostaglandin I_2 signaling licenses Treg suppressive function and prevents pathogenic reprogramming

Allison E. Norlander, … , Talal A. Chatila, R. Stokes Peebles Jr.

J Clin Invest. 2021;131(7):e140690. https://doi.org/10.1172/JCI140690.

Research Article | Immunology | Inflammation

Graphical abstract

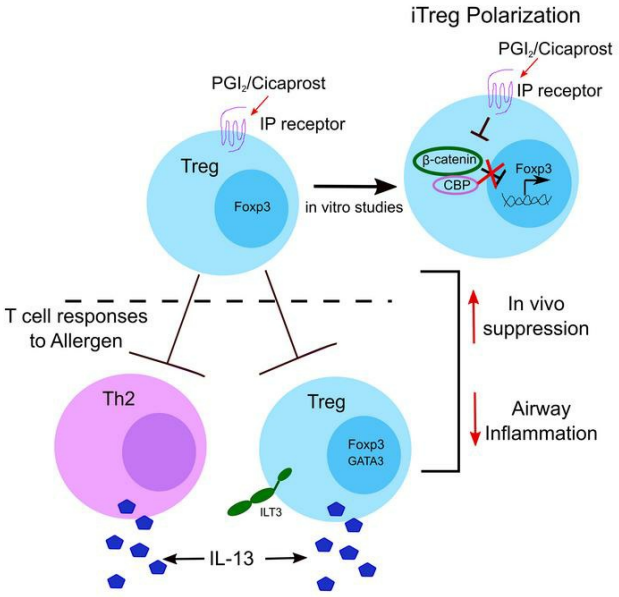

Prostaglandin I_2 signaling licenses Treg suppressive function and prevents pathogenic reprogramming

Allison E. Norlander,[1] Melissa H. Bloodworth,[1] Shinji Toki,[1] Jian Zhang,[1] Weisong Zhou,[1] Kelli Boyd,[2] Vasiliy V. Polosukhin,[1] Jacqueline-Yvonne Cephus,[1] Zachary J. Ceneviva,[1] Vivek D. Gandhi,[1] Nowrin U. Chowdhury,[2] Louis-Marie Charbonnier,[3] Lisa M. Rogers,[4] Janey Wang,[5] David M. Aronoff,[2,4,6] Lisa Bastarache,[5] Dawn C. Newcomb,[1,2] Talal A. Chatila,[3] and R. Stokes Peebles Jr.[1,2,7]

[1]Division of Allergy, Pulmonary, and Critical Care Medicine and [2]Department of Pathology, Microbiology, and Immunology, Vanderbilt University School of Medicine, Nashville, Tennessee, USA. [3]Division of Immunology, Boston Children's Hospital, Department of Pediatrics, Harvard Medical School, Boston, Massachusetts, USA. [4]Division of Infectious Diseases, Department of Medicine, [5]Department of Biomedical Informatics, and [6]Department of Obstetrics and Gynecology, Vanderbilt University Medical Center (VUMC), Nashville, Tennessee, USA. [7]United States Department of Veterans Affairs, Nashville, Tennessee, USA.

Tregs restrain both the innate and adaptive immune systems to maintain homeostasis. Allergic airway inflammation, characterized by a Th2 response that results from a breakdown of tolerance to innocuous environmental antigens, is negatively regulated by Tregs. We previously reported that prostaglandin I_2 (PGI_2) promoted immune tolerance in models of allergic inflammation; however, the effect of PGI_2 on Treg function was not investigated. Tregs from mice deficient in the PGI_2 receptor IP (IP KO) had impaired suppressive capabilities during allergic airway inflammatory responses compared with mice in which PGI_2 signaling was intact. IP KO Tregs had significantly enhanced expression of immunoglobulin-like transcript 3 (ILT3) compared with WT Tregs, which may contribute to the impairment of the IP KO Treg's ability to suppress Th2 responses. Using fate-mapping mice, we reported that PGI_2 signaling prevents Treg reprogramming toward a pathogenic phenotype. PGI_2 analogs promoted the differentiation of naive T cells to Tregs in both mice and humans via repression of β-catenin signaling. Finally, a missense variant in IP in humans was strongly associated with chronic obstructive asthma. Together, these data support that PGI_2 signaling licenses Treg suppressive function and that PGI_2 is a therapeutic target for enhancing Treg function.

Introduction

Tregs are important components of the adaptive immune system that promote tolerance, prevent the development of autoimmune diseases, and suppress inflammation (1, 2). Tregs are characterized by their expression of the canonical transcription factor Forkhead box p3 (Foxp3), which is essential for their development and function (3, 4). Mutations in Foxp3 are associated with Treg deficiency and have been linked to systemic autoimmunity and allergic disease (5–8). Thymically derived Tregs (tTregs) develop in the thymus and are released as functional Tregs, whereas peripheral or inducible Tregs (iTregs) develop extrathymically from $CD4^+$ naive T cells in the presence of antigen and TGF-β (9).

Allergy and asthma affect over 300 million people globally and cause substantial morbidity and mortality, revealing the need for new therapeutics (10, 11). Tregs are present in the lungs during type 2 inflammation and are critical for the suppression of allergic inflammation (12–15). In this setting, Tregs express GATA-binding protein 3 (GATA3) and interferon regulatory factor 4 (IRF4) in order to specifically suppress Th2 effector cells (16–18). Recent studies demonstrated that a subset of lung Tregs may undergo pathogenic reprogramming during allergic inflammation and asthma as a result of increased expression of GATA3 and activation of the Wnt and Hippo pathways (19, 20). These Tregs subsequently lose Foxp3 expression and begin to express type 2 inflammatory cytokines, thus promoting disease (19, 20). Furthermore, a subset of Tregs that express immunoglobulin-like transcript 3 (ILT3) have been described (21, 22). ILT3 is a potent inhibitory receptor and has been shown to induce anergy in T cells (23). $ILT3^+$ Tregs are unable to inhibit Th2 responses as a result of their inability to control the maturation of IRF4 and programmed cell death 1 ligand 2 (PD-L2) double-positive ($IRF4^+PD\text{-}L2^+$) DCs, a Th2-promoting subset (21, 22). In our study, we investigated the impact of the prostaglandin I_2 (PGI_2) signaling pathway on ILT3 expression and Treg stability in vivo. The knowledge described here may have therapeutic importance in enhancing Treg function and promoting immune tolerance.

PGI_2 is an arachidonic acid metabolite produced through the cyclooxygenase pathway that signals through a G protein–coupled receptor, termed IP (24–26). We and others have reported that mice genetically deficient in the PGI_2 receptor IP (IP KO) have enhanced allergic airway inflammation (27–31). Moreover, IP KO mice had a defect in immune tolerance in an airway allergen-challenge model, revealing that PGI_2 receptor signaling is essential for immune tolerance in this system (32). These results strongly suggested that (a) endogenous PGI_2 signaling is an essential component of immunologic tolerance in the setting of allergic inflammation and (b) PGI_2

Conflict of interest: The authors have declared that no conflict of interest exists.

Submitted: May 26, 2020; **Accepted:** January 27, 2021; **Published:** April 1, 2021.
Reference information: *J Clin Invest*. 2021;131(7):e140690.
https://doi.org/10.1172/JCI140690.

may be a therapeutic strategy for enhancing or restoring immune tolerance (32–34). Based on our previous finding that PGI_2 signaling is essential for immune tolerance and that Tregs are a critical component of immune tolerance, we hypothesized that PGI_2 signaling promotes Treg function. Herein, we show that PGI_2 signaling enhanced Foxp3 expression in Tregs from mice, promoted Treg suppressive function in vivo in murine allergen-challenge models, was critical for Treg stability, and inhibited ILT3 expression on Tregs in vivo. Moreover, we show that PGI_2 signaling increased human Treg differentiation in vitro via β-catenin. These studies reveal that PGI_2, approved by the FDA for the treatment of pulmonary hypertension, is an important pharmacologic agent that enhances Treg function and differentiation, thus having potential therapeutic implications for allergic airway inflammation.

Results

PGI_2 signaling critically promotes tTreg function in vivo in an airway allergen-challenge model. Based on our previously published work demonstrating that PGI_2 signaling promotes tolerance, we hypothesized that PGI_2 signaling through IP promotes Treg function in vivo. We and others have previously reported expression of IP by $CD4^+$ T cells (29, 33–35). We sought to determine the approximate stage during development at which T cells begin to express IP. We found that only CD4 single-positive thymocytes express IP compared with thymocytes at all other developmental stages (Supplemental Figure 1; supplemental material available online with this article; https://doi.org/10.1172/JCI140690DS1). Next, we began to test the aforementioned hypothesis, examining the suppressive capacity of IP KO tTregs in an airway allergen-challenge model. In our experiments, we utilized *Foxp3*^{EGFP} BALB/c reporter mice that coexpress GFP and Foxp3 downstream of the *Foxp3* promoter and that can be used to identify Tregs and assess Foxp3 expression. We crossed *Foxp3*^{EGFP} mice with *DO11.10*$^+$ mice that express a transgenic T cell receptor (TCR) specific for the ovalbumin (OVA) peptide. These crosses generated mice in which GFP^+ Tregs expressed a TCR specific for OVA, the allergen used in the adoptive transfer model. The presence of the OVA-specific TCR in the setting of OVA challenge allowed the transferred Tregs to traffic to the site of inflammation and respond in an antigen-specific fashion. Our reasoning for using an OVA-based model was 2-fold: numerous tools are available to transferred Tregs, and Tregs are important for control of OVA-induced inflammation (36, 37). We subsequently crossed the *DO11.10*$^+$×*Foxp3*^{EGFP} onto an IP deficient (IP KO) background in order to determine the impact of PGI_2 signaling on the function of the OVA-specific adoptively transferred Tregs. Therefore, we had mice that had OVA-specific $CD4^+$ cells that expressed GFP under the control of the Foxp3 promoter on either an IP-intact (*DO11.10*$^+$×*Foxp3*^{EGFP}) or an IP KO (*DO11.10*$^+$×*Foxp3*^{EGFP}×IP KO) background. To examine the effect of PGI_2 signaling on tTreg function during allergic airway inflammation, we utilized RAG1-deficient (*Rag1*$^{-/-}$) mice, which lack both T and B cells, as recipient mice in an adoptive transfer model of allergic airway inflammation. In order for the *Rag1*$^{-/-}$ mice to develop an allergic response, it was necessary to adoptively transfer antigen-specific effector $CD4^+$ T cells. In addition, some mice also received adoptively transferred tTregs from either the IP-intact or IP KO backgrounds of reporter mice described above to assess their suppressive function. Effector T cells (Teffs) were isolated from *DO11.10*$^+$ mice so the differences in suppression seen could be attributable to differences in functionality between tTregs in which IP signaling was intact (IP-intact tTregs) and IP KO tTregs. The *Rag1*$^{-/-}$ recipients were then allergen challenged according to the schematic in Figure 1A. Mice that received only adoptively transferred Teffs and that were OVA challenged had significantly more IL-13 in the bronchoalveolar lavage fluid (BAL) (Figure 1B) in addition to significantly more $KJ126^+CD4^+IL\text{-}13^+$ OVA-specific cells (Figure 1C) than mice that received only adoptively transferred Teffs and were not OVA challenged, signifying that OVA challenge induced allergic inflammation. The gating strategy for Figure 1 is shown in Supplemental Figure 2. Total numbers of cells were calculated using hemocytometer-based counts and population percentages from set flow cytometry gates described in the gating strategy. Mice that received only adoptively transferred Teffs had significantly greater IL-13 in the BAL as well as lung $KJ126^+CD4^+IL\text{-}13^+$ OVA-specific T cells compared with mice that received adoptively transferred Teffs + IP-intact tTregs (Figure 1, B and C). These data revealed that adoptively transferred tTregs in which IP signaling is intact inhibited allergic inflammation. There was no difference in IL-13 in the BAL or in $KJ126^+CD4^+IL\text{-}13^+$ OVA-specific T cells between mice that received adoptively transferred Teffs + IP KO tTregs and mice that received only adoptively transferred Teffs, revealing a suppressive defect in IP KO tTregs. Importantly, there was a significant increase in these endpoints compared with those in mice that received adoptively transferred Teffs + IP-intact tTregs (Figure 1, B and C). These results signify that tTregs from IP KO mice had a defect in suppressive function compared with tTregs from mice in which PGI_2 signaling was intact. Importantly, the total number of lung-infiltrating tTregs, identified as OVA-specific $KJ126^+$*Foxp3*$^{EGFP+}CD25^+$ cells, was not different between mice that received adoptively transferred Teffs + IP-intact tTregs or IP KO tTregs (Figure 1D), demonstrating that impaired trafficking was not the cause of the differences in in vivo suppression between these groups. Taken together, these data show that PGI_2 signaling in tTregs was critical for protection from allergen challenge–induced inflammation.

PGI_2 signaling promotes tTreg Foxp3 expression. As lack of PGI_2 signaling impairs tTreg suppression in an in vivo allergen-challenge model, we next hypothesized that IP KO tTregs had impaired function in the absence of disease stimulus compared with tTregs from WT mice (WT tTregs). To test this hypothesis, we first assessed the level of Foxp3 expression in WT tTregs and IP KO tTregs. Previous studies have shown that Foxp3 MFI in Tregs correlated with suppressive capability (38, 39). We stained total splenocytes from WT and IP KO mice for Foxp3. The gating strategy for Figure 2A is shown in Supplemental Figure 3. We found that, while the percentage of tTregs among splenocytes was unchanged, tTregs from IP KO mice consistently had a significantly lower Foxp3 MFI than tTregs from WT mice, suggesting the IP KO tTregs may be less functional (Figure 2, A and B, and Supplemental Figure 4A). Moreover, IP KO tTregs produced significantly less IL-10 than WT tTregs after 3 days of activation on anti-CD3– and anti-CD28–coated plates (Figure 2C). Together, these data show that PGI_2 signaling contributes to Foxp3 expression within tTregs and suggest that absence of PGI_2 signaling

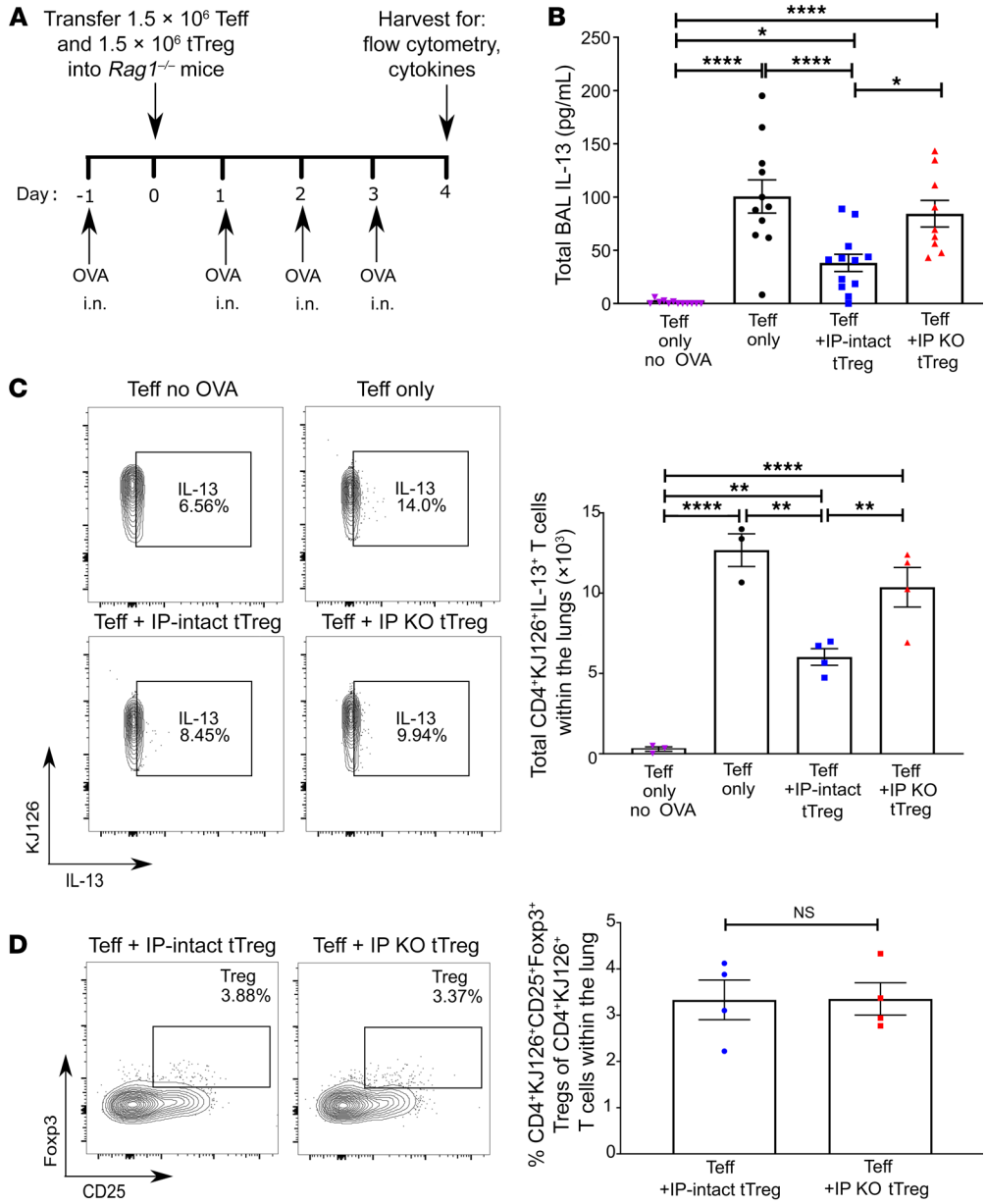

Figure 1. PGI_2 signaling critically promotes tTreg function in vivo in an airway allergen-challenge model. (**A**) Experimental schematic. (**B**) BAL IL-13 as measured by ELISA (n = 9–12, 3 independent experiments combined). (**C**) Representative flow cytometric analysis and calculated total cell number of $CD4^+KJ126^+IL\text{-}13^+Foxp3^-$ T cells present in the lungs (n = 3–4, 1 experiment shown that is representative of the results from 2 other independent experiments). (**D**) Representative flow cytometric analysis and plotted population percentages of $CD4^+KJ126^+CD25^+Foxp3^+$ Tregs present in the lungs (n = 4, 1 experiment shown that is representative of the results from 2 other independent experiments). Data are represented as mean ± SEM. Statistical significance was determined by 1-way ANOVA (**B** and **C**) and Student's 2-tailed t test (**D**). $^*P < 0.05$; $^{**}P < 0.01$; $^{****}P < 0.0001$.

alters tTreg functionality. Importantly, at baseline, there were no differences in total numbers or percentages of Tregs between WT or IP KO in either the lungs or spleen (Supplemental Figure 4, A and B). In addition, there were no differences between WT and IP KO Tregs utilizing an in vitro suppression assay (data not shown). Further, there were no differences between WT and IP KO Tregs with respect to levels of CD25 expression or expression of the Treg markers CTLA4, ICOS, PD1, GITR, Helios, CD39, or CD73 (Supplemental Figure 4C). These data would suggest that stress or an inflammatory state is necessary for eliciting measurable functional differences between WT and IP KO Tregs.

PGI_2 signaling enhances iTreg function in vivo in the setting of allergic airway inflammation. Based on our finding that PGI_2 signaling promoted tTreg function in vivo, we next hypothesized that IP KO iTregs are similarly less suppressive in vivo than iTregs in which IP signaling is intact. To test this hypothesis, we utilized immunocompetent WT BALB/c recipient mice instead of *Rag1*$^{-/-}$ mice to determine whether adoptively transferred IP KO iTregs have suppressive defects in a host with its own compartment of Tregs compared with adoptively transferred iTregs in which IP signaling is intact. The WT recipient mice were sensitized intraperitoneally with a solution of OVA mixed with aluminum hydroxide (alum) and later challenged with nebulized OVA to trigger allergic airway inflammation. Naive $CD4^+$ T cells from *DO11.10*$^+$×*Foxp3*^{EGFP} and *DO11.10*$^+$×*Foxp3*^{EGFP}×IP KO mice were isolated and cultured on anti-CD3–coated plates with IL-2 and TGF-β to polarize them to iTregs prior to transfer. WT recipient mice were challenged with nebulized OVA according to the schematic detailed in Figure 3A. OVA-sensitized and -challenged WT mice (OVA WT) had significantly more IL-5 and IL-13 (Figure 3B), total cells (Figure 3C), and total eosinophils (Figure 3D) in BAL than nonsensitized and nonchallenged WT mice, signifying OVA challenge–induced allergic inflammation. OVA WT mice that received adoptively transferred *DO11.10*$^+$×*Foxp3*^{EGFP} iTregs had significantly lower IL-5 and IL-13, significant-

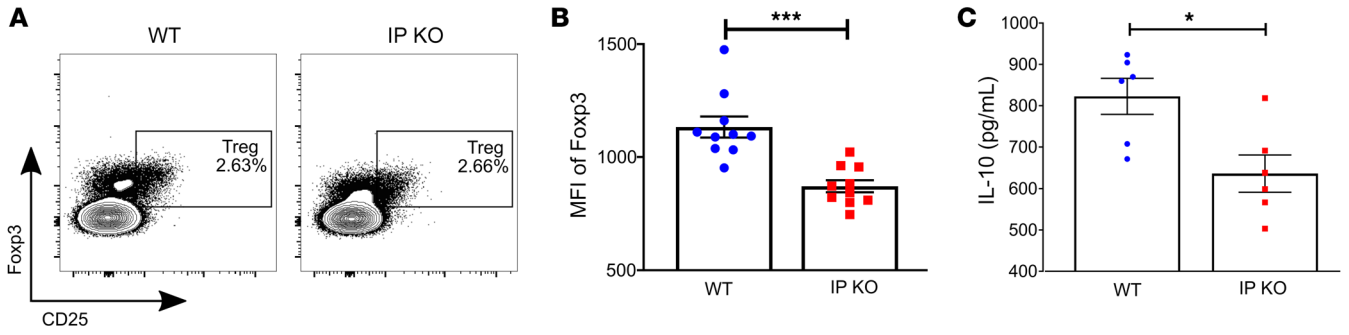

Figure 2. PGI_2 signaling promotes tTreg Foxp3 expression. (**A**) Representative flow cytometric analysis of $CD4^+CD25^+Foxp3^+$ Tregs from the spleens of IP KO or WT mice (n = 10, 2 independent experiments combined). (**B**) MFI of Foxp3 from gated Treg population (n = 10, 2 independent experiments combined). (**C**) Quantification of IL-10 produced by cultured purified tTregs (n = 6, 2 independent experiments combined). Data are represented as mean ± SEM. Statistical significance was determined by Student's t test. $^*P < 0.05$; $^{***}P < 0.001$.

ly fewer total cells, and a trend toward fewer eosinophils in the BAL than OVA WT mice that did not receive transferred iTregs (Figure 3, B–D). A pathologist blinded to the treatment groups performed individual lung scoring for major basic protein (MBP) staining to examine infiltrating eosinophils. OVA WT mice that received adoptively transferred *DO11.10*$^+$×*Foxp3*^{EGFP} iTregs exhibited reduced eosinophil infiltration (Figure 3E) compared with OVA WT mice. These data demonstrated that iTregs in which IP signaling is intact inhibited allergic inflammation. There were no differences between OVA WT mice and OVA WT mice that received adoptively transferred *DO11.10*$^+$×*Foxp3*^{EGFP}×IP KO iTregs in IL-5 and IL-13, total cells, and eosinophils in the BAL, nor in eosinophil infiltration into the lungs, revealing a defect in the suppressive function of iTregs from IP KO mice. However, OVA WT mice adoptively transferred *DO11.10*$^+$×*Foxp3*^{EGFP}×IP KO iTregs had significantly more IL-5 and IL-13, total cells, and eosinophils in BAL as well as eosinophil infiltration into the lungs than OVA WT mice adoptively transferred DO11.10×*Foxp3*^{EGFP} iTregs (Figure 3, C–E). These data demonstrate that iTregs in which IP signaling is intact inhibit the progression of inflammation and injury that results from allergen challenge, while IP KO iTregs do not. We next evaluated by flow cytometry the number of type 2 cytokine-expressing $CD4^+$ T cells present within the lungs from a separate set of mice that underwent the identical adoptive transfer protocol (Figure 3A). Prior to performing these studies, we crossed *Foxp3*^{EGFP} mice onto congenic CD45.1 BALB/c mice to be used as WT recipient mice for these studies. It is important to note that BALB/c mice have the CD45.2 allele; therefore, both *DO11.10*$^+$×*Foxp3*^{EGFP} and *DO11.10*$^+$×*Foxp3*^{EGFP} ×IP KO mice express CD45.2. These WT $CD45.1^+$ recipient mice were generated in order to differentiate between adoptively transferred iTregs that came from *DO11.10*$^+$×*Foxp3*^{EGFP} or *DO11.10*$^+$×*Foxp3*^{EGFP}×IP KO mice that expressed CD45.2 and host Tregs. OVA WT mice had significantly more $IL\text{-}13^+CD45.1^+CD4^+$ T cells and $IL\text{-}5^+CD45.1^+CD4^+$ T cells ($P < 0.05$) than nonsensitized and nonchallenged WT mice, indicating that OVA challenge induced type 2 cytokine-producing $CD4^+$ cells, as expected. The gating strategy for Figure 3 is shown in Supplemental Figure 5. Total numbers of cells were calculated using hemocytometer-based counts and population percentages from set flow cytometry gates. OVA WT mice with adoptively transferred *DO11.10*$^+$×*Foxp3*^{EGFP} iTregs or *DO11.10*$^+$×*Foxp3*^{EGFP}×IP KO iTregs had significantly fewer $IL\text{-}13^+$ $CD45.1^+CD4^+$ T cells compared with OVA WT mice without transferred iTregs (Figure 3F). Importantly, there were significantly fewer $IL\text{-}13^+CD45.1^+CD4^+$ T cells in OVA WT mice with adoptively transferred *DO11.10*$^+$×*Foxp3*^{EGFP} iTregs compared with OVA WT mice with adoptively transferred *DO11.10*$^+$×*Foxp3*^{EGFP}×IP KO iTregs (Figure 3F), revealing that IP KO iTregs were not able to suppress cellular expression of this type 2 cytokine as effectively as WT iTregs. There was no difference in the total number of lung-infiltrating iTregs between OVA WT mice with adoptively transferred *DO11.10*$^+$×*Foxp3*^{EGFP} iTregs and *DO11.10*$^+$×*Foxp3*^{EGFP}×IP KO iTregs (Figure 3G). Together, these data demonstrate that IP KO iTregs, similarly to IP KO tTregs, are functionally impaired and unable to inhibit allergen-induced inflammation as well as iTregs in which IP signaling is intact.

PGI_2 signaling promotes iTreg differentiation in vitro. Since adoptively transferred IP KO iTregs are dysfunctional in vivo, we further hypothesized that naive T cells from IP KO mice have impaired ability to differentiate to iTregs compared with naive T cells from WT mice. To test this hypothesis, we polarized both WT and IP KO naive T cells to iTregs in vitro using IL-2 and TGF-β on anti-CD3–coated plates. IP KO naive T cells demonstrated an impaired ability to polarize to IP KO iTregs compared with WT naive T cells. Specifically, after culture, there were fewer IP KO cells that were $Foxp3^{EGFP+}CD25^+$, which we classify as iTregs, compared with similarly polarized WT cells (Figure 4, A and B). The gating strategy for Figure 4, A and B, is shown in Supplemental Figure 6. Furthermore, we found that IP KO iTregs produced significantly less IL-10 than WT iTregs after polarization (Figure 4C). However, there were no differences between WT and IP KO iTregs utilizing an in vitro suppression assay (data not shown). Taken together, these data show that PGI_2 signaling contributes to iTreg differentiation and function and suggest that absence of this signaling results in an iTreg that is less functional.

PGI_2 signaling promotes Treg stability during allergic inflammation. Recent literature demonstrates that lung Tregs may lose Foxp3 expression, resulting in production of type 2 cytokines that contribute to allergic inflammation (19). Based on our data suggesting that IP KO Tregs are less stable due to their reduced Foxp3 MFI at baseline, we hypothesized that the stability of IP KO Tregs

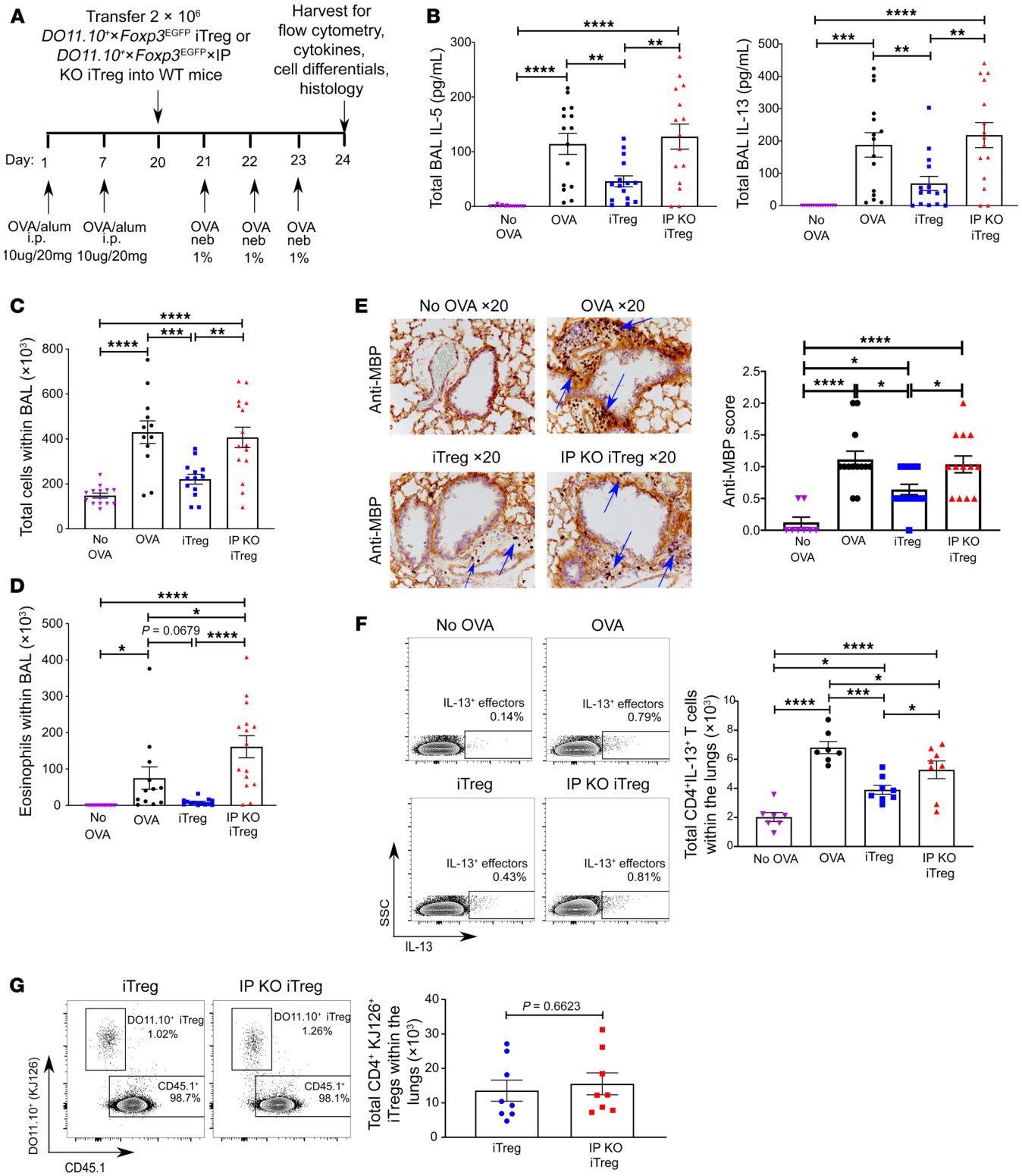

Figure 3. PGI_2 signaling enhances iTreg function in vivo in the setting of allergic airway inflammation. (**A**) Experimental schematic. (**B**) Total BAL IL-5 and IL-13 (n = 15, 3 independent experiments combined). (**C**) Total cells within BAL (n = 10–15, 3 independent experiments combined). (**D**) Eosinophils within BAL (n = 10–15, 3 independent experiments combined). (**E**) Anti-MBP score and representative histological images (n = 8–15, 3 independent experiments combined). (**F**) Representative flow cytometric analysis and calculated total cell number of IL-13$^+$CD4$^+$ T cells within the lungs (n = 7–8, 2 independent experiments combined). (**G**) Representative flow cytometric analysis and calculated total cell number of CD4$^+$KJ126$^+$ iTregs that were transferred in as sorted Foxp3$^+$CD25$^+$ iTregs (n = 8, 2 independent experiments combined). Data are represented as mean ± SEM. Statistical significance was determined by 1-way ANOVA (**C**–**G**). *P < 0.05; **P < 0.01; ***P < 0.001; ****P < 0.0001.

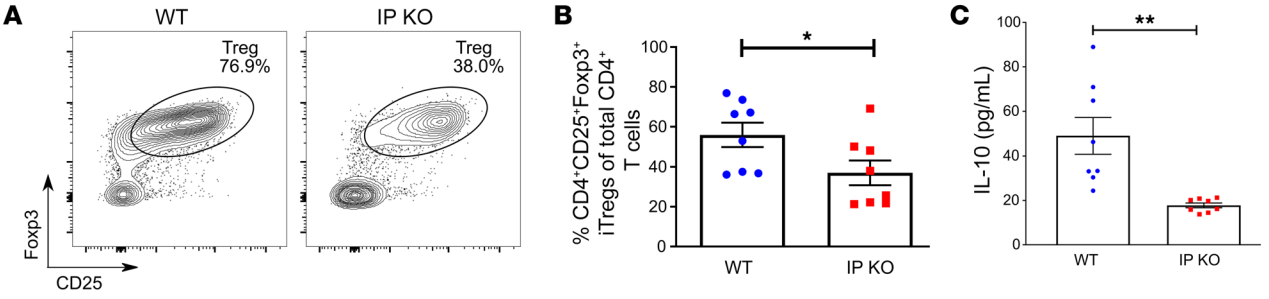

Figure 4. PGI_2 signaling promotes iTreg differentiation in vitro. (**A**) Representative image of a flow cytometry plot of iTregs present in culture after naive WT or IP KO T cells were activated with anti-CD3 and differentiated using IL-2 and TGF-β (n = 8, 3 independent experiments combined). (**B**) Plotted percentages of WT and IP KO polarized iTregs (n = 8, 3 independent experiments combined). (**C**) Amount of IL-10 produced by differentiated iTregs (n = 8, 3 independent experiments combined). Data are represented as mean ± SEM. *P < 0.05; **P < 0.01.

is impaired during allergic inflammation. We generated fate-mapping mice for these experiments. Mice in these experiments were either WT (*Foxp3*^{EGFPcre}×*Rosa26*$^{YFP/YFP}$×*IL-13*^{tdtomato}) or IP KO (IP KO×*Foxp3*^{EGFPcre}×*Rosa26*$^{YFP/YFP}$×*IL-13*^{tdtomato}). In these mice, any cell that was ever Foxp3$^+$ expresses yellow fluorescent protein (YFP), those currently Foxp3$^+$ express GFP, and those currently IL-13$^+$ express tdTomato. The lung cells of these mice were examined by flow cytometry after OVA sensitization and challenge. Current Tregs were defined as GFP$^+$YFP$^+$, while ex-Tregs, or T cells that once expressed and have lost Foxp3 expression, were GFP$^-$YFP$^+$. We found that OVA sensitization and challenge increased Tregs in the lungs of both WT and IP KO mice compared with nonchallenged controls. Interestingly, there was a significantly increased number of both Tregs and ex-Tregs in the lungs of sensitized and challenged IP KO mice compared with WT mice (Figure 5, A–C). The gating strategy for Figure 5 is shown in Supplemental Figure 7. Total numbers of cells were calculated using hemocytometer-based counts and population percentages from set flow cytometry gates. Furthermore, we found that OVA sensitization and challenge increased the total numbers of lung IL-13$^+$ Tregs and IL-13$^+$ ex-Tregs in both WT and IP KO mice compared with nonsensitized and nonchallenged controls. Importantly, OVA sensitization and challenge significantly increased total numbers of lung IL-13$^+$ Tregs and ex-Tregs in IP KO mice compared with OVA-sensitized and -challenged WT mice (Figure 5, D–G). Together, these data suggest that IP KO Tregs are less stable and more prone to reprogramming toward a pathogenic IL-13–expressing Treg phenotype during allergic inflammation than WT Tregs. We also show that OVA-sensitized and -challenged IP KO mice have more IL-13$^+$Th2 cells than OVA-sensitized and -challenged WT mice (Figure 5H and Supplemental Figure 8). Strikingly, the Treg/Th2 ratio within the lungs of OVA-sensitized and -challenged IP KO mice was significantly lower than in WT mice (Figure 5I). These data suggest that, although IP KO mice have more Tregs within their lungs, there are fewer Tregs for every Th2 cell present compared with those in WT mice, making it more difficult for IP KO Tregs to suppress Th2 cell function in this in vivo model. It is important to note that the stability of IP KO Tregs is potentially impacted by the enhanced inflammatory state (increased cytokine levels) occurring within the IP KO mouse as a result of the presence of dysfunctional Tregs. These data demonstrate that PGI_2 signaling in Tregs may play a role in their ability to maintain their suppressive and functional state during inflammatory conditions.

PGI_2 signaling inhibits the expression of ILT3 on Tregs. Several recent studies have demonstrated that Tregs expressing ILT3 did not suppress Th2 responses due to their inability to suppress the development of a DC subset (PD-L2$^+$IRF4$^+$) that promotes the formation of Th2 cells (21, 22, 40, 41). ILT3 functions as a repressor of TCR signaling (21). Upregulation of ILT3 on Tregs has been shown in 3 previous studies to result in their inability to restrain Th2 responses in vivo (21, 22, 42). We therefore hypothesized that IP KO Tregs express increased ILT3 based on our findings that both IP KO tTregs and iTregs exhibited impaired suppressive capability in vivo. We found that lung IP KO Tregs isolated from mice sensitized and challenged with OVA expressed significantly greater *ILT3* mRNA and *GATA3* mRNA than WT Tregs (Figure 6, A and B). Additionally, we found a significant increase in the percentage of ILT3$^+$GATA3$^+$ Tregs in the lungs isolated from OVA IP KO mice compared with OVA WT mice (Figure 6, C and D). The gating strategy for Figure 6, C and D, is shown in Supplemental Figure 9. Concomitantly, we found a significantly increased percentage of PD-L2$^+$IRF-4$^+$ DCs in the lungs of OVA IP KO mice compared with OVA WT mice (Figure 6, E and F). The gating strategy for Figure 6, E and F, is shown in Supplemental Figure 10. Together, these data show that PGI_2 signaling is critical in inhibiting ILT3 expression on Tregs.

PGI_2 signaling promotes iTreg differentiation and prevents tTreg destabilization. Thus far, we have examined the effects of endogenous PGI_2 signaling on Treg functionality. It is also important to determine the role exogenous PGI_2 has on Treg function. We hypothesized that exogenous PGI_2 enhances murine Treg function. To test this hypothesis, we first examined the effect of cicaprost, a PGI_2 analog, on the iTreg polarization of CD4$^+$ cells from WT mice. We found that increasing doses of cicaprost significantly promoted iTreg polarization, as measured by flow cytometry (Figure 7A). iTregs were identified using the gating strategy shown in Supplemental Figure 6. Next, to study the impact of exogenous PGI_2 on tTregs in vitro, we utilized an in vitro polarization protocol that entails the use of high levels of cytokines present during an allergic response, IL-4 and IL-33. IL-4 promotes GATA3 expression and Th2 polarization, while IL-33 is an epithelial-derived cytokine that promotes type 2 responses (22, 43). Additionally, IL-2 was added to the culture, as it is critical for the maintenance and function of

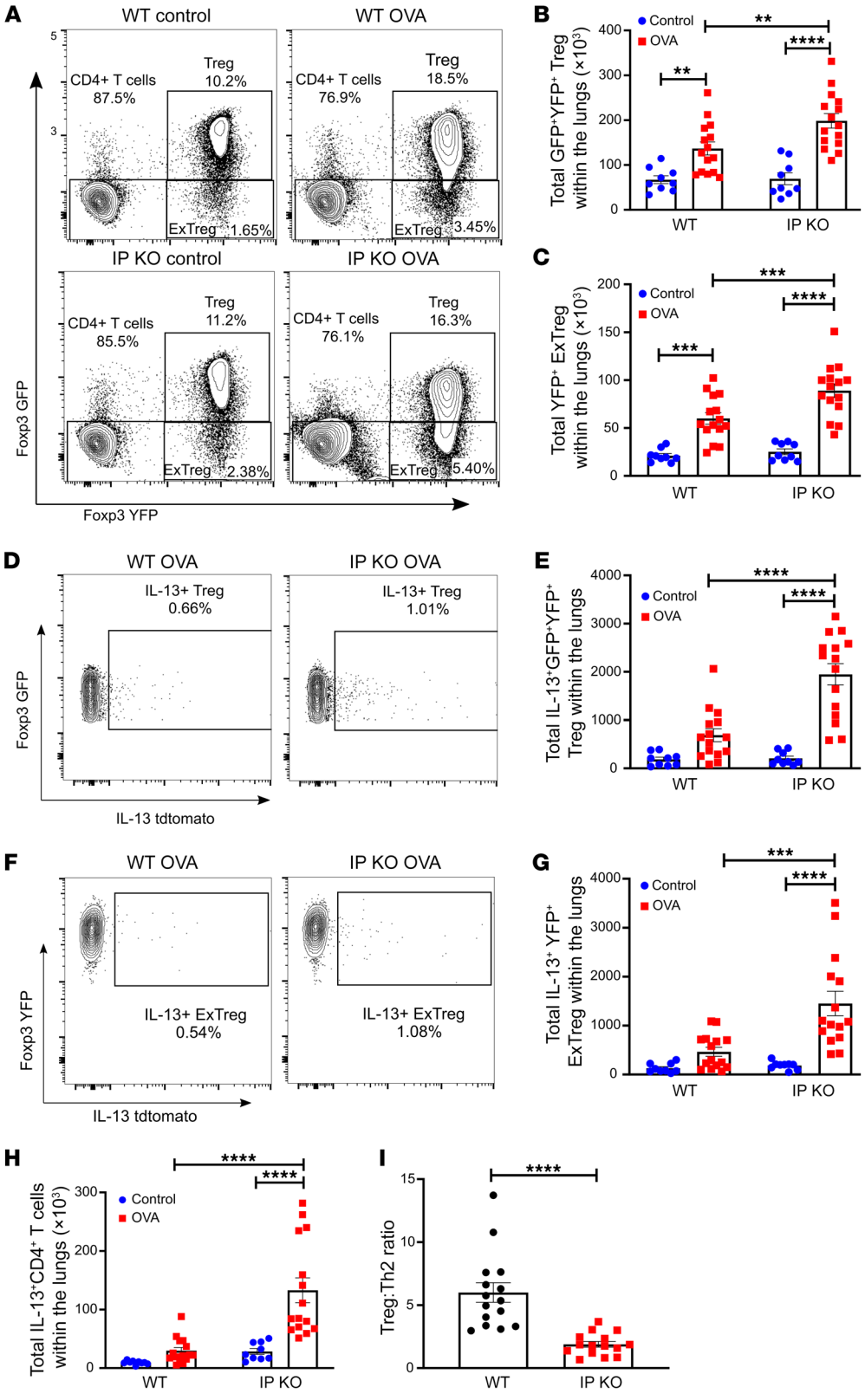

Figure 5. PGI_2 signaling promotes Treg stability during allergic inflammation. In these experiments, WT and IP KO mice were sensitized and challenged with OVA and the presence of Tregs in the lung was analyzed. (**A**) Representative flow cytometric analysis of Foxp3GFP$^+$YFP$^+$ Tregs and Foxp3YFP$^+$ ex-Tregs (n = 9–15, 3 independent experiments combined). (**B**) Calculated total cell number of Foxp3GFP$^+$YFP$^+$ Tregs within the lungs (n = 9-15, 3 independent experiments combined). (**C**) Calculated total cell number of Foxp3YFP$^+$ ex-Tregs within the lungs (n = 9–15, 3 independent experiments combined). (**D**) Representative flow cytometric analysis of IL-13$^+$Foxp3GFP$^+$YFP$^+$ Tregs (n = 9–15, 3 independent experiments combined). (**E**) Calculated total cell number of IL-13$^+$Foxp3GFP$^+$YFP$^+$ Tregs within the lungs (n = 9–15, 3 independent experiments combined). (**F**) Representative flow cytometric analysis of IL-13$^+$Foxp3YFP$^+$ ex-Tregs (n = 9–15, 3 independent experiments combined). (**G**) Calculated total cell number of IL-13$^+$Foxp3YFP$^+$ ex-Tregs within the lungs (n = 9–15, 3 independent experiments combined). (**H**) Calculated total cell number of IL-13$^+$CD4$^+$ Th2 cells within the lungs (n = 9–15, 3 independent experiments combined). (**I**) Calculated Treg/Th2 ratio (n = 9–15, 3 independent experiments combined). Data are represented as mean ± SEM. Statistical significance was determined by 2-way ANOVA (**A**–**G**) and Student's 2-tailed t test (**I**). $^{**}P < 0.01$; $^{***}P < 0.001$; $^{****}P < 0.0001$.

Tregs (44, 45). tTregs were polarized with IL-2, IL-4, and IL-33 for 6 days on anti-CD3– and anti-CD28–coated plates. We hypothesized that exogenous PGI_2 signaling promotes the stability of Tregs, measured through maintenance of Foxp3 expression. We indeed found that cicaprost prevented tTreg destabilization, defined as a loss of Foxp3 expression as a result of stimulus with high levels of IL-4 and IL-33. Significantly greater percentages of WT tTregs were present after 6 days in culture with high levels of IL-2, IL-4, and IL-33 when treated with cicaprost compared with vehicle treatment (Figure 7B). tTregs were defined according to the gating strategy shown

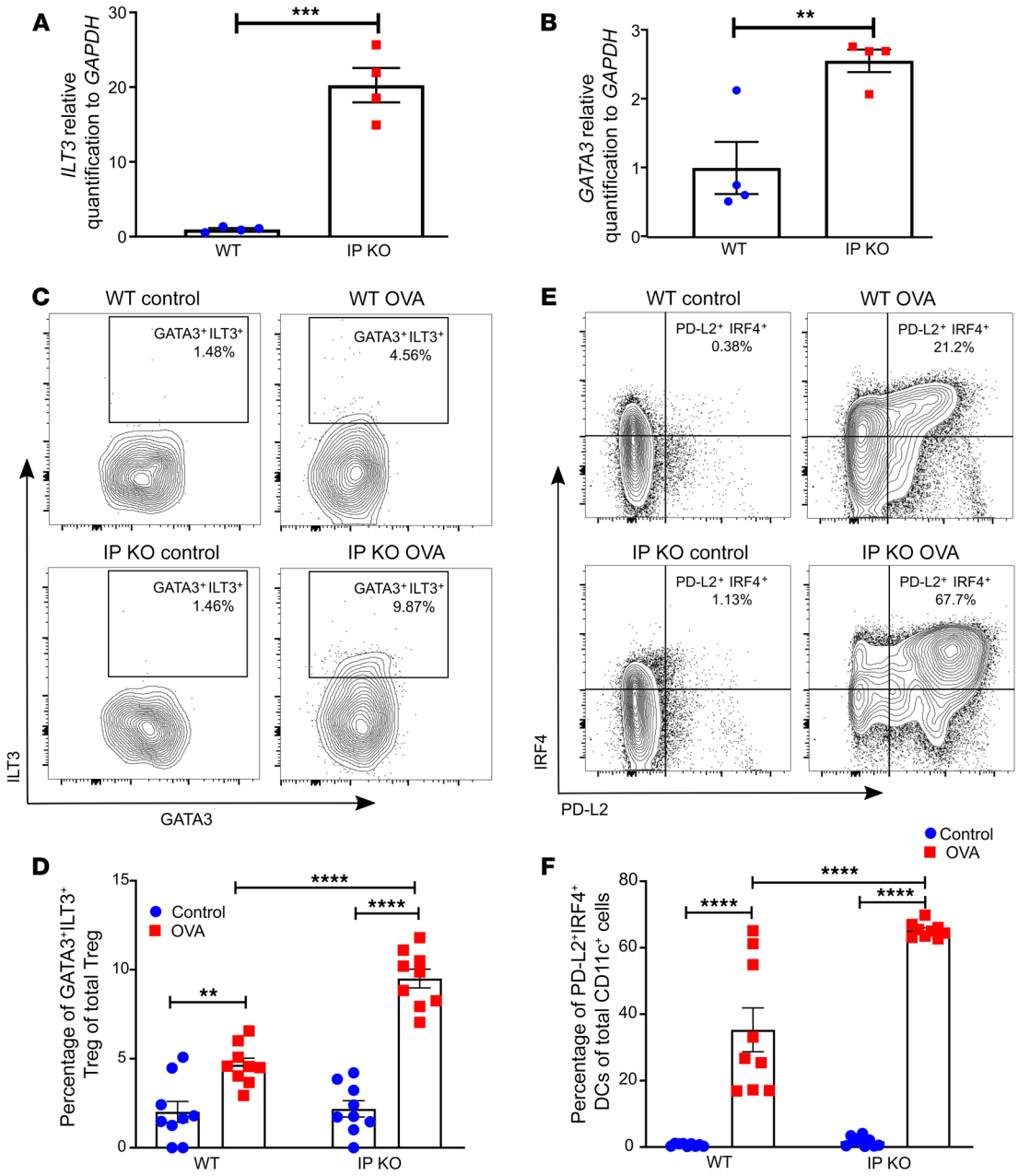

Figure 6. PGI_2 signaling inhibits the expression of ILT3 on Tregs. (**A**) Relative quantification of *ILT3* mRNA from isolated Tregs from OVA-sensitized and -challenged lungs normalized to *GAPDH* (n = 4, 1 independent experiment). (**B**) Relative quantification of *GATA3* mRNA from isolated Tregs from OVA-sensitized and -challenged lungs normalized to *GAPDH* (n = 4, 1 independent experiment). (**C**) Representative flow cytometric analysis of ILT3$^+$GATA3$^+$ Tregs in the lungs of OVA-sensitized and -challenged WT and IP KO mice (n = 9, 2 independent experiments combined). (**D**) Plotted population percentages of ILT3$^+$GATA3$^+$ Tregs (n = 9, 2 independent experiments combined). (**E**) Representative flow cytometric analysis of IRF4$^+$PD-L2$^+$ DCs in the lungs of OVA-sensitized and -challenged WT and IP KO mice (n = 9, 2 independent experiments combined). (**F**) Plotted population percentages of IRF4$^+$PD-L2$^+$ DCs (n = 9, 2 independent experiments combined). Data are represented as mean ± SEM. Statistical significance was determined by 2-way ANOVA (**D** and **F**) and Student's 2-tailed t test (**A** and **B**). $^{**}P < 0.01$; $^{***}P < 0.001$; $^{****}P < 0.0001$.

in Supplemental Figure 11. This result shows that cicaprost treatment enhances the stability of WT tTregs in vitro. Thus far, we have demonstrated that exogenous PGI_2 promoted Treg function and stability in vitro; however, whether exogenous PGI_2 promotes Treg function in vivo was an important unaddressed question. To examine this possibility, we infused a different PGI_2 analog, treprostinil, into WT mice for a duration of 2 weeks through use of osmotic mini pumps. We chose to use treprostinil in vivo because it is more heat stable and thus more suitable for long-term infusion studies. The top dose in our curve, 45 ng/kg/min, was chosen based on the average dose used in patients with pulmonary hypertension (46–49). We found that this dose of treprostinil significantly increased the percentage of Foxp3$^+$ cells within the lung (Figure 7C). Foxp3$^+$ cells were identified using the gating strategy shown in Supplemental Figure 12. These data show that exogenous PGI_2 signaling promoted the formation and stability of Tregs.

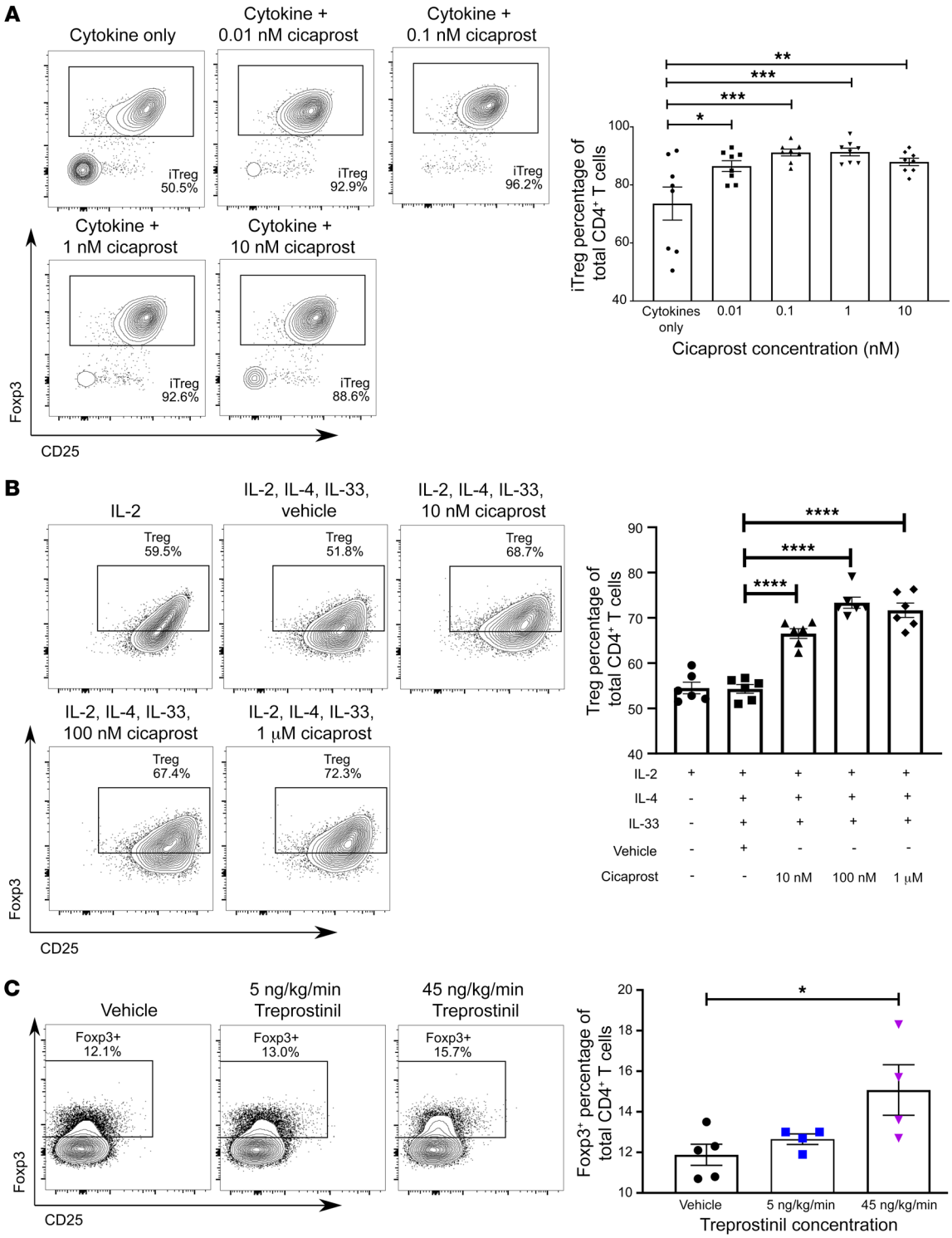

Figure 7. PGI_2 signaling promotes iTreg differentiation and prevents tTreg destabilization. (**A**) Representative flow cytometric analysis and plotted percentage of polarization to iTregs after purified naive T cells were cultured with IL-2 and TGF-β and increasing doses of cicaprost (n = 8, 2 independent experiments combined). (**B**) Representative flow cytometric analysis and plotted Treg percentages after 6 days in culture and treatment with IL-2, IL-4, IL-33, and increasing doses of cicaprost (n = 6, 2 independent experiments combined). (**C**) Representative flow cytometric analysis and representative plotted population percentages of Foxp3⁺ Treg within the lung after treprostinil treatment (n = 4–5, 1 experiment shown that is representative of the results from one other independent experiments). Data are represented as mean ± SEM. Statistical significance was determined by 1-way ANOVA. $^*P < 0.05$, $^{**}P < 0.01$, $^{***}P < 0.001$, $^{****}P < 0.0001$

PGI_2 analogs promote human Treg differentiation via repression of β-catenin signaling. Finally, we examined the effect of PGI_2 analogs on the formation of Tregs from human donors. Based on our mouse data, we hypothesized that cicaprost treatment increases the percentage of iTregs following polarization of $CD4^+$ T cells isolated from the peripheral blood of humans compared with vehicle treatment. We indeed found that cicaprost dose-dependently significantly increased $CD4^+$ T cell polarization to iTregs, as measured by flow cytometry (Figure 8, A and B). iTregs were defined using the gating strategy shown in Supplemental Figure 13. These data are plotted as percentage of baseline such that all treated conditions are normalized to the cytokine condition for the specific individual to account for intrinsic variability in iTreg differentiation. Furthermore, we found that there was a concomitant significant increase in Foxp3 MFI following cicaprost treatment (Figure 8C). These data demonstrate that PGI_2 signaling critically promotes human Treg differentiation from $CD4^+$ T cells. We next determined the signaling pathway responsible for PGI_2-induced enhanced Treg polarization. We chose to evaluate PKA, exchange factor directly activated by cAMP (EPAC), and Wnt/β-catenin signaling. We have previously shown that PKA signaling is important for PGI_2's suppression of Th1 and Th2 cell cytokine production, and PGI_2 has repeatedly been shown to signal via cAMP (25, 34). PGI_2 has not been shown to signal through EPAC in any T cell subsets; however, it has been demonstrated to do so in both smooth muscle cells and endothelial cells (50, 51). Thus far, no studies directly link PGI_2 to β-catenin activation; however, a recent study demonstrated that Wnt signaling mediated by β-catenin promoted Th2 cell–like reprogramming of Tregs in models of allergic inflammation and asthma (20). Additionally, a separate study linked β-catenin expression to ILT3 expression on Tregs (21). To determine which of these pathways is downstream of PGI_2 in Tregs, we polarized human $CD4^+$ T cells in the presence of 3 different inhibitors. We utilized the PKA inhibitor H89, the EPAC inhibitor ESI09, and ICG001, which inhibits the interaction between β-catenin and the cAMP-responsive element (CREB) binding protein (CBP). These data are plotted as percentage of baseline such that all treated conditions are normalized to the vehicle (DMSO or EtOH) condition for the specific individual inhibitor to account for intrinsic variability in iTreg differentiation. We found that both H89 and ESI09 had no effect on Treg differentiation, as both failed to inhibit the cicaprost-induced enhanced polarization of $CD4^+$ T cells to Tregs (Figure 8, E and F), leading us to conclude that PGI_2 signals independently of both PKA and EPAC in Tregs. However, ICG001 increased Treg polarization when given at a concentration of 1 μM and addition of cicaprost resulted in no further increase in Treg polarization (Figure 8D). These data demonstrate that PGI_2 signaling represses β-catenin activation and signaling in conjunction with CBP, resulting in enhanced Treg formation.

PTGIR missense variant is associated with chronic obstructive asthma with exacerbation in humans. Based on our in vivo findings in a mouse model of asthma and our in vitro results revealing that PGI_2 signaling critically promotes Treg function, we determined whether polymorphisms of IP in humans (gene name *PTGIR*) were associated with asthma. Therefore, we investigated the association of asthma phenotypes and subtypes in genetic variants in a population of 25,363 individuals genotyped in Vanderbilt's biobank, BioVU (52). These subjects were genotyped on the Exome BeadChip, an Illumina genotyping platform designed to capture coding variants. This cohort allowed us to examine associations between genetic variants in the coding region of *PTGIR* and asthma. In our cohort, only 1 variant in *PTGIR* — p.P226T (rs138619017) — had a sufficient number of heterozygotes (≥100) to test for association. *PTGIR* p.P226T is a missense mutation that is located in the third intracellular loop of IP in an area that has been shown to interact with the heterotrimeric G protein (53). We tested to determine whether there was an association between this variant and either asthma or asthma subtypes using Phecodes. We found that the *PTGIR* p.P226T variant was significantly associated with both Phecode 495.1, "chronic obstructive asthma," and Phecode 495.11, "chronic obstructive asthma with exacerbation," as shown in Table 1. Furthermore, using the UK Biobank summary statistics in Gene Atlas (54), we found that *PTGIR* p.P226T was significantly associated with asthma ($P = 0.016$; odds ratio = 1.23; cases = 52,296, controls = 399,995; allele frequency 0.0036). These results from 2 different biobanks suggest that a missense mutation in the PGI_2 receptor may be a risk factor for asthma.

Discussion

We describe a role for PGI_2 signaling in promoting Treg stability, function, and differentiation. tTregs from IP KO mice were less suppressive in an immunodeficient adoptive transfer-based model of allergic inflammation than tTregs from mice in which PGI_2 signaling was intact. Additionally, iTregs from IP KO mice were less suppressive in an immunocompetent adoptive transfer-based model of allergic inflammation than iTregs generated from WT mice. As there were no differences in total number of infiltrating Tregs within the lungs in either set of experiments, the impairment in suppression was not due to inability of IP KO Tregs to effectively traffic to the lungs. Instead, IP KO Tregs were unable to adequately prevent the proliferation of Th2 cells in response to OVA. As a whole, the data from the adoptive transfer experiments parse the effects of PGI_2 signaling within Tregs and Th2 during allergic inflammation and demonstrate that PGI_2 signaling in Tregs is critical for maintenance of the cells' suppressive function during allergic inflammation. In vitro studies revealed that tTregs from IP KO mice had a lower Foxp3 MFI than tTregs from WT mice and produced less IL-10 upon nonspecific stimulation. Naive T cells from IP KO mice were less able to polarize to iTregs, and subsequently, these iTregs produced less IL-10 than iTregs generated from WT mice. Importantly, more Tregs from IP KO mice were $ILT3^+GATA3^+$ and were less stable and more prone to conversion to $IL\text{-}13^+$ Tregs or ex-Tregs than Tregs from WT mice. Exogeneous PGI_2 promoted Treg formation in vivo and in vitro while it additionally promoted Treg stability in vitro. Finally, exogenous PGI_2 also promoted the formation of human iTregs via repression of β-catenin signaling.

IP KO Tregs displayed decreased stability during disease progression. Using fate-mapping mice, we observed that greater numbers of IP KO Tregs lost Foxp3 expression and began expressing the proinflammatory cytokine IL-13 during the course of disease compared with WT mice, effectively becoming reprogrammed in the allergic microenvironment. Other studies have linked increased expression of GATA3 to enhanced reprogramming and thereby

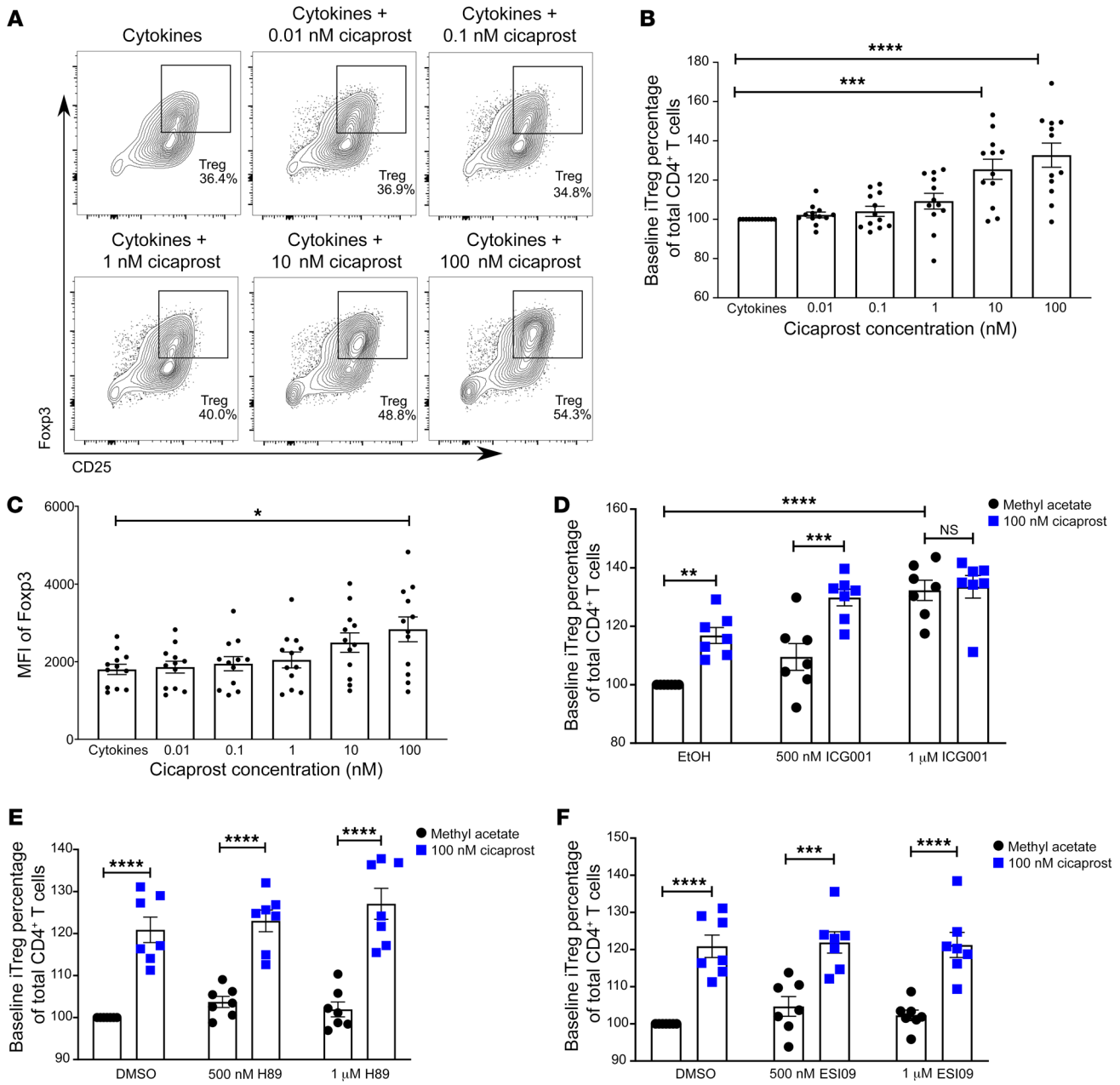

Figure 8. PGI_2 analogs promote human Treg differentiation. Purified $CD4^+$ T cells were cultured with IL-2 and TGF-β and increasing doses of cicaprost. (**A**) Representative flow cytometric analysis ($n = 12$). (**B**) Baseline-normalized percentage polarization to iTregs ($n = 12$). (**C**) MFI ($n = 12$). In a separate set of experiments, purified $CD4^+$ T cells were cultured with IL-2, TGF-β, cicaprost, and inhibitors to different signaling pathways. (**D**) Purified $CD4^+$ T cells were treated with 2 different concentrations of ICG001, a β-catenin inhibitor. Baseline-normalized percentage polarization to iTregs is plotted ($n = 7$, 3 independent experiments combined). (**E**) Purified $CD4^+$ T cells were treated with 2 different concentrations of H89, a PKA inhibitor. Baseline-normalized percentage polarization to iTregs is plotted ($n = 7$, 3 independent experiments combined). (**F**) Purified $CD4^+$ T cells were treated with 2 different concentrations of ESI09, an EPAC inhibitor. Baseline-normalized percentage polarization to iTregs is plotted ($n = 7$, 3 independent experiments combined). Data are represented as mean ± SEM. Statistical significance was determined by 1-way ANOVA or 2-way ANOVA. $^*P < 0.05$; $^{**}P < 0.01$; $^{***}P < 0.001$; $^{****}P < 0.0001$.

formation of ex-Tregs (22, 36). The increased presence of ex-Tregs found in the lungs of IP KO mice compared with WT during allergic inflammation is likely due to increased GATA3 expression in IP KO Tregs compared with WT Tregs. However, IP KO mice exist in an elevated inflammatory state compared with WT mice when allergically challenged. This increased inflammation and abundance of Th2 cytokines, allowed as a result of dysfunctional IP KO Tregs, may also be affecting IP KO Treg stability. Future studies are needed to uncover whether one or both of the aforementioned scenarios are affecting Treg stability in IP KO mice.

IP KO Tregs had enhanced expression of ILT3 and GATA3 compared with WT Tregs during disease progression. Upregulation of ILT3 on Tregs resulted in Treg inability to restrain Th2 responses in mouse models of airway inflammation and autoimmune gastritis in vivo (21, 22, 42). Together, these studies along with the data reported here reveal the importance of evaluating

Table 1. Association test of Phecodes for asthma and asthma-subtypes analysis of PTGIR variant p.P226T

rsID	Amino acid change	Effect allele	Allele frequency	Phecode	jd_string	Cases	Controls	Heterozygote cases	Heterozygote controls	OR	*P* value
rs138619017	p.P226T	T	0.00301	495	Asthma	1,886	23,477	17	134	1.58	0.085
rs138619017	p.P226T	T	0.00301	495.1	Chronic obstructive asthma	226	23,477	6	134	4.73	2.3×10^{-03}
rs138619017	p.P226T	T	0.00301	495.11	Chronic obstructive asthma with exacerbation	43	23,477	3	134	12.90	2.0×10^{-03}
rs138619017	p.P226T	T	0.00301	495.2	Asthma with exacerbation	316	23,477	2	134	1.11	0.702

Association testing was conducted using Fisher's exact test with Bonferroni's correction. OR, odds ratio.

Tregs for expression of ILT3 to determine their functional capacity during the progression of Th2-mediated diseases. Elevated ILT3 expression on IP KO Tregs compared with WT Tregs further revealed the enhanced existence of a dysregulated Treg population in IP KO mice that are less able to control type 2 inflammation. ILT3 expression on Tregs could be an additional marker of Treg exhaustion. Currently, Treg exhaustion can be denoted by their expression levels of PD1, LAG3, or ICOS (55). In one study, aberrant PD1 expression on Tregs present in Treg-specific tumor suppressor liver kinase B1 (LKB1) deficient mice, which naturally acquire fatal autoimmune disease, denoted the existence of an exhausted Treg population (56). The authors went on to show that upregulation of PD1 expression on LKB1-deficient Tregs was linked to their inability to control Th2 responses as well as the accumulation of PD-L2$^+$ DCs (56). This exaggerated type 2 response seen with elevated PD1 expression on Tregs is similar to what occurs when increased populations of Tregs express ILT3 (21, 22, 42, 56). It is therefore possible that ILT3 expression on Tregs results in a similar exhausted phenotype.

Notably, PGI_2 analogs enhanced Treg differentiation both in vitro and in vivo in mice and in vitro in human T CD4$^+$ cells, revealing the importance of PGI_2 signaling to human Treg formation. This effect in human cells was shown to be mediated by β-catenin; however, no studies directly link PGI_2 to β-catenin activation. However, prostaglandin E_2 (PGE_2), also an arachidonic acid metabolite like PGI_2, activated β-catenin (57). A recent study linked Wnt signaling and activation of β-catenin with the promotion of Th2 reprogramming of Tregs in models of allergic disease and asthma (20). Interestingly, a different study linked β-catenin expression to ILT3 expression within Tregs; however, this study showed that cells with lower expression of β-catenin had higher levels of ILT3 (21). This is the opposite of what we would expect, given our findings and those of others (20). Moreover, to date, inhibitors of β-catenin improved immune responses to different types of cancers (58). As β-catenin signaling promotes Th2 signaling over Th1, in addition to repressing the formation of tTregs, development of a Treg-specific therapy may be warranted (59, 60).

To determine the relevance of PGI_2 signaling to asthma in humans, we found that a variant in the human *PTGIR* gene was strongly associated with chronic obstructive asthma with exacerbation in a BioVU cohort. An association with the same variant and asthma was confirmed in the UK Biobank with an effect size consistent with what was observed in BioVU. The Genome Wide Association Studies (GWAS) catalog, a compiled resource of significant associations found in GWAS, reports that common SNPs in and near *PTGIR* have been associated with ulcerative colitis and inflammatory bowel disease. Although large GWASs of asthma have been conducted, no associations between SNPs within *PTGIR* and asthma have been reported (61–63). However, because GWAS typically only tests for associations with common genetic variants, this does not preclude the possibility that rare coding variants in human genetic variation in *PTGIR* affect the risk of asthma. Given that our findings in BioVU are based on a rare variant, these results should be interpreted with caution. However, these data are suggestive that there are genetic variants in *PTGIR* present in the human population that influence asthma risk, perhaps similarly to how a SNP in the PGI_2 pathway was associated with increased risk of cardiovascular diseases (64). Our data do not reveal that the association of chronic obstructive asthma with *PTGIR*–p.P226T is attributable to a defect in Treg function or any other cell type. However, it is tempting to speculate that individuals with SNPs in the PGI_2 pathway that result in lower production of PGI_2 or impaired IP signaling exhibit impaired Treg suppressive capacity, not only predisposing them to the development of cardiovascular disease, but also to autoimmune and allergic diseases. Importantly, prospective studies will be necessary to confirm the functional nature of association.

Very little is known about how PGI_2 signaling regulates Treg function and stability. Our study is the first, to our knowledge, to directly investigate the direct effect of PGI_2 signaling on the Treg itself in vivo in the context of allergic inflammation. Investigators have previously shown that treating OVA-pulsed DCs with iloprost prior to injection into DC-depleted mice inhibited production of Th2 cytokines and increased IL-10 secretion from OVA-specific T cells after subsequent OVA aerosol challenge (65). However, these investigators did not identify whether the IL-10–secreting cells were Tregs, nor did they investigate the signaling mechanisms leading to IL-10 production (65). A separate set of investigators demonstrated that culture of naive T cells with iloprost promoted Th17 while suppressing Treg differentiation under their respective skewing conditions, via a cAMP-mediated mechanism (66). These results are the opposite of our results in that we demonstrate that PGI_2 analogs enhance Treg differentiation; however, we went further and validated that PGI_2 signaling promotes Treg function in vivo. Models of Treg deficiency in

relation to the development of pulmonary hypertension have also been investigated. Female rats developed more severe pulmonary hypertension than males when lacking Tregs, and it was ultimately discovered that Tregs promoted plasma expression of PGI_2 and cardiopulmonary expression of PGI_2 synthase (PTGIS) and protected rats from the development of pulmonary hypertension (67). Moreover, in vitro human Tregs increased concentrations of PGI_2 and IL-10 when in culture with human cardiac microvascular cells (67). This study evaluated the importance of Tregs for protection against pulmonary hypertension, but did not directly examine the impact of PGI_2 on Tregs. Additionally, iloprost-treated DCs promoted Treg differentiation and protected mice from the development of allergic inflammation (68). The effect of PGI_2 on Tregs published in this study was mediated by DCs and was not due to a direct effect of PGI_2 on Tregs. We believe our study is unique in that the effects described are a result of PGI_2 signaling within the Tregs. Furthermore, a group of investigators found that Tregs express PTGIS that is acetylated by CBP/p300, leading to increased production of PGI_2 by Tregs compared with naive T cells (69). We were unable to confirm expression of PTGIS within Tregs by Western blot or PCR (Supplemental Figure 14). Interestingly, Castillo et al. were unable to find a direct effect of the PGI_2 analog iloprost on Treg differentiation and concluded that CBP/p300 functions upstream of IP receptor stimulation and that increased production of endogenous PGI_2 mediates the effect of PTGIS on Treg differentiation via CBP/p300 (69). However, our data would suggest the opposite, that PGI_2 stimulation of IP results in β-catenin activation, leading to its complexing with its transcriptional coactivator CBP, which results in enhanced Treg differentiation. As a whole, Castillo et al.'s overarching conclusion that PGI_2 as well as CBP/p300 signaling is important for Treg differentiation supports our findings (69).

In conclusion, our results strongly suggest that PGI_2 signaling licenses Treg suppressive function and prevents reprogramming toward a pathogenic Treg phenotype. The possibility that PGI_2 signaling promotes Treg function has tremendous therapeutic implications, as it would signify that PGI_2 may be the first pharmacologic agent that increases Treg function in vivo. PGI_2 has been FDA approved to treat pulmonary hypertension for 3 decades (70). Therefore, a PGI_2 analog could be repurposed to increase the ability of Treg to suppress allergic inflammation or other inflammatory diseases, such as autoimmunity.

Methods

Mice

BALB/c (BALB/cAnNCrl) mice were obtained from Charles River. *Rag1*$^{-/-}$ (C.129S7(B6)-*Rag1*^{tm1Mom}/J), *DO11.10*$^{+}$ (C.Cg-Tg(DO11.10)10Dlf/J), *Foxp3*^{EGFP} (C.Cg-*Foxp3*^{tm2Tch}/J), and CD45.1 (CByJ.SJL(B6)-*Ptprc*^{a}/J) mice, all on a BALB/c genetic background and all *Ptgir*$^{+/+}$, were obtained from Jackson Laboratory. IP KO (*Ptgir*$^{-/-}$) mice were provided by Garret FitzGerald (University of Pennsylvania, Philadelphia, Pennsylvania, USA) as a gift and were backcrossed 10 generations onto BALB/c. *Foxp3*^{EGFP} (*Ptgir*$^{+/+}$) mice were crossed with IP KO mice to generate *Foxp3*^{EGFP}×IP KO (*Ptgir*$^{-/-}$) mice. *DO11.10*$^{+}$ (*Ptgir*$^{+/+}$) mice were crossed onto *Foxp3*^{EGFP} and IP KO×*Foxp3*^{EGFP} mice to generate *DO11.10*$^{+}$×*Foxp3*^{EGFP} (*Ptgir*$^{+/+}$) and *DO11.10*$^{+}$×*Foxp3*^{EGFP}×IP KO (*Ptgir*$^{-/-}$) mice, respectively. *Foxp3*^{EGFPcre}×*Rosa26*$^{YFP/YFP}$ mice were provided in house. *IL-13*^{tdtomato} mice were provided as a gift from Andrew McKenzie (Medical Research Council Laboratory of Molecular Biology, Cambridge, United Kingdom). Both of these strains are also *Ptgir*$^{+/+}$. *IL-13*^{tdtomato} mice were crossed with *Foxp3*^{EGFPcre}×*Rosa26*$^{YFP/YFP}$ mice to generate *Foxp3*^{EGFPcre}×*Rosa26*$^{YFP/YFP}$×*IL-13*^{tdtomato} (*Ptgir*$^{+/+}$) mice; these mice were then crossed with IP KO Mice to generate IP KO×*Foxp3*^{EGFPcre}×*Rosa26*$^{YFP/YFP}$×*IL-13*^{tdtomato} (*Ptgir*$^{-/-}$) mice. Female mice, ages 7–12 weeks, were used in experiments.

Allergic sensitization/challenge

Mice were sensitized at day 0 and day 7 with 100 μL of OVA (10 μg) and alum (20 mg) solution intraperitoneally. On days 21 to 23, BALB/c mice were challenged through the airway with nebulized 1% OVA to elicit allergic airway inflammation.

BAL

Immediately after euthanasia, mice were immobilized, and the trachea was isolated and cleaned using forceps. A small incision was made in the trachea into which an endotracheal tube was inserted; 800 μL of saline was instilled into the lungs of mice and then aspirated from the airways using the same syringe.

Lung single-cell suspension

Immediately after euthanasia, mice were immobilized, and both lungs were harvested. Lungs were placed into 1 mL of RPMI + 5% FBS and subsequently minced to fine pieces. Lungs were then digested for 25 minutes at 37°C and ground on a 70 μM strainer and washed with RPMI + 5% FBS. Lung cells were centrifuged,and RBCs were lysed with RBC Lysis Buffer (Tonbo Biosciences) and run over a second 70 μM filter.

Splenic and thymic single-cell suspension

Immediately after euthanasia, spleen and/or thymus was harvested, ground on a 70 μM filter, and washed through with RPMI. Cells were spun down; RBCs were lysed using RBC Lysis Buffer (Tonbo Biosciences) and then filtered through a second 70 μM filter.

tTreg adoptive transfer model

Rag1$^{-/-}$ mice were anesthetized using isoflurane and intranasally challenged with 5 mg/mL OVA on days –1 and days 1 to 3. On day 0, single-cell suspensions of spleens were prepared from *DO11.10*$^{+}$, *DO11.10*$^{+}$×*Foxp3*^{EGFP}, and *DO11.10*$^{+}$×*Foxp3*^{EGFP}×IP KO mice. Naive T cells were isolated from *DO11.10*$^{+}$ single-cell suspensions, and Tregs were isolated from *DO11.10*$^{+}$×*Foxp3*^{EGFP} and *DO11.10*$^{+}$×*Foxp3*^{EGFP}×IP KO mice using magnetic beads technology (Miltenyi Biotec). Appropriate numbers of cells were administered to mice anesthetized with ketamine/xylazine through the tail vein.

Histology

Immediately after euthanasia, mice were immobilized, and the right lung was ligated and excised. Then, 600 μL of 10% formalin was injected into the left lung via the endotracheal tube, as described above. The endotracheal tube was then removed, and the trachea was quickly tied off below the incision. The inflated left lung was then harvested and placed in 5 mL of 10% formalin at 4°C for 48 hours. The lungs were then embedded, cut, and stained for MBP. Lungs were then scored based on intensity of the stain.

ELISA

BAL fluid was evaluated using an IL-13 Quantikine ELISA (R&D Systems). Treg cell culture supernatant was evaluated using an IL-10 Quantikine ELISA (R&D systems).

Flow cytometry

Anti-mouse antibodies used for flow cytometry are listed in Supplemental Table 2. Anti-human antibodies used for flow cytometry are listed in Supplemental Table 3. Intracellular staining was performed in one of two ways: (a) if the cells contained a fluorescent reporter, cells were fixed using a 1:2 dilution of 10% phosphate-buffered formalin for 40 minutes, permeabilized using permeabilization buffer (eBioscience), and then stained; or (b) in all other experiments, cells were fixed and permeabilized using the Foxp3/Transcription Factor Staining Buffer Set (eBioscience). Live/dead discrimination was performed using Ghost Dye Violet 510 (Tonbo Biosciences), Ghost Dye Red 710 (Tonbo Biosciences), or LIVE/DEAD Near-IR (Invitrogen) on both human and mouse cells. Cells were analyzed on a BD LSR II Cell Analyzer (BD Biosciences) or a Cytek Aurora (Cytek Biosciences), and the data were analyzed using FlowJo (BD Biosciences). Flow cytometry experiments were analyzed in the VUMC Flow Cytometry Shared Resource.

T cell culture

Treg culture. Splenic single-cell suspensions from *Foxp3*^{EGFP} and *Foxp3*^{EGFP}×IP KO mice were enriched for CD4$^+$ T cells using magnetic bead technology (Miltenyi Biotec). Cells were then stained, and CD4$^+$CD25$^+$ *Foxp3*$^{EGFP+}$ Tregs were isolated using FACS technology on a BD FACS Aria III Cell Sorter. Tregs were then plated at 100,000 cells/well on 96-well plates precoated with 1 μg/mL anti-CD3 and 0.5 μg/mL anti-CD28 (BD Biosciences). Tregs were supplemented with 100 IU of human IL-2 (NIH) and allowed to incubate at 37°C for 3 days. Media was later evaluated for the presence of IL-10 by ELISA (IL-10 Mouse Quantikine ELISA Kit, R&D Systems). In a separate set of experiments, 20,000 Tregs/well were supplemented with combinations of 1000 IU of human IL-2 (NIH), 100 ng/mL IL-33 (Peprotech), and 100 ng/mL IL-4 (Peprotech) in addition to indicated doses (10 nm to 1 μM) of cicaprost (Cayman Chemical) for 6 days in round-bottom plates with CD3/CD28 T cell activation beads (Invitrogen Dynabeads). Media was supplemented on day 4. On day 6, the presence of CD4$^+$CD25$^+$ *Foxp3*$^{EGFP+}$ cells was evaluated.

iTreg polarization. Splenic single-cell suspensions from *Foxp3*^{EGFP} and *Foxp3*^{EGFP}×IP KO mice were enriched for CD4$^+$ T cells using magnetic bead technology (Miltenyi Biotec). Cells were then stained, and CD4$^+$CD62L$^+$ naive T cells were isolated using FACS technology on a BD FACS Aria III Cell Sorter. Naive T cells were then plated at 100,000 cells/well on 96-well plates precoated with 1 μg/mL anti-CD3 (BD Biosciences). Naive T cells were supplemented with 100 IU/mL human IL-2 (NIH) and 10 ng/mL human TGF-β (Peprotech); in some experiments, indicated doses (0.01–100 nM) of cicaprost (Cayman Chemical) were also added. Naive T cells were polarized at 37°C for 4 days and then evaluated for the presence of CD4$^+$CD25$^+$ *Foxp3*$^{EGFP+}$ Tregs by flow cytometry. Media was later evaluated for the presence of IL-10 by ELISA (IL-10 Mouse Quantikine ELISA Kit, R&D Systems).

Th2 polarization. Splenic cell suspensions from WT mice were enriched for CD4$^+$CD62L$^+$ naive T cells using bead technology (Miltenyi Biotec). Naive T cells were supplemented with 10 ng/mL mouse IL-4 (Peprotech) and 1 0μg/mL mouse anti–IFN-γ (R&D Systems).

Th0 polarization. Splenic cell suspensions from WT mice were enriched for CD4$^+$CD62L$^+$ naive T cells using bead technology (Miltenyi Biotec). Naive T cells were plated as is with no supplementation.

iTreg adoptive transfer model

BALB/c mice were sensitized at day 0 and day 7 with 100 μL of OVA (10 μg) and Alum (20 mg) solution intraperitoneally. On day 16, *DO11.10*$^+$×*Foxp3*^{EGFP} or *DO11.10*$^+$×*Foxp3*^{EGFP}×IP KO naive T cells were isolated from splenic cell suspensions using magnetic bead technology. Naive T cells were polarized in 24-well plates in the same manner as described above. On day 20, CD4$^+$CD25$^+$*Foxp3*$^{EGFP+}$ iTregs were isolated from both WT and IP KO cultures by FACS. Sensitized BALB/c mice were anesthetized with ketamine/xylazine, and the appropriate number of cells was administered to mice through the tail vein. On days 21–23, BALB/c mice were challenged through the airway with nebulized 1% OVA.

Real-time PCR

Tregs were purified using FACS. mRNA was extracted using the RNeasy Micro Kit (QIAGEN) according to the manufacturer's instructions. Aorta were isolated from mice. RNA was extracted from mouse aorta using TRIzol and the RNeasy Mini Kit (QIAGEN) according to the manufacturer's instructions. RNA was converted to cDNA using the High Capacity cDNA Reverse Transcription Kit (Applied Biosystems) according to the manufacturer's instructions. All target probes were obtained from TaqMan (Applied Biosystems), and targets were preamplified using the TaqMan PreAmp Master Mix Kit (Applied Biosystems). Targets included the following: *GATA3* (Applied Biosystems, TaqMan, Mm00484683_m1), *ILT3* (Applied Biosystems, TaqMan, Mm01614371_m1), *PTGIS* (Applied Biosystems, TaqMan, Mm01248013_m1), and *GAPDH* (Applied Biosystems, TaqMan, Mm99999915_g1). All samples were run and analyzed using a QuantStudio 12k Flex.

Western blot

Isolated Tregs and mouse aorta were lysed in RIPA buffer containing protease inhibitor and phosphatase inhibitor. Lysates were denaturized with 4× laemmli sample buffer including DTT on a heating block at 95°C for 5 minutes. The lysates were separated by SDS-PAGE using 12.5% Mini-PROTEAN TGXTM Precast Gel (Bio-Rad). Separated protein was transferred to nitrocellulose membranes using the iBlot Transfer Stack, nitrocellulose, mini, and the iBlot Dry Blotting System (Thermo Fisher Scientific). The membrane was blocked with Odyssey Blocking Buffer (LI-COR Biosciences) for 2 hours, incubated overnight at 4°C with the primary antibodies (PTGIS [3C8], Cayman Chemical, 10247) (β-actin [I-19], Santa Cruz Biotechnology Inc., SC-1616), and then further incubated for 1 hour with the primary antibody-matched secondary antibodies (donkey anti-rabbit IRDye 680LT and donkey anti-goat IRDye 800CW, LI-COR Biosciences). The stained membrane was scanned and analyzed by Odyssey imaging system (LI-COR Biosciences).

Mini-pump implantation

14 day osmotic mini-pumps (Alzet) were loaded with either vehicle or treprostinil (United Therapeutics Corp.) for a targeted administration of 45 ng/kg/min based on weight. Mice were anesthetized using ketamine/xylaxine. A small incision was made in the back of the mouse at the base of the neck, and the mini-pumps were implanted subcutaneously. Mice received appropriate analgesic at the time of surgery.

Human samples

Demographic details of the subject population are defined in Supplemental Table 1.

iTreg polarization. CD4+ T cells were isolated from whole blood using the RosetteSep Human CD4+ T cell Enrichment Cocktail Kit (StemCell). CD4+ T cells were polarized to iTregs in the same way as mouse, described above, only using anti-human CD3 (BD Biosciences) to coat the plate, 200 IU/mL human IL-2, and 1 μg/mL soluble anti-human CD28 (BD Biosciences). The inhibitors H89, ICG001, and ESI09 were purchased from Cayman Chemical and were used at the indicated doses (500 nM to 1 μM).

Variant analysis

The genotyped cohort comprised 25,363 individuals of European ancestry (determined by principle components) in Vanderbilt's BioVU cohort. The cohort was genotyped on the Exome BeadChip by Illumina, which was designed to capture functional exonic variants. Of the 11 *PTGIR* variants genotyped on the Exome BeadChip, only one — rs138619017, p.P226T — had a high enough allele frequency to do association testing (≥100 heterozygotes/homozygotes for the minor allele). We used Phecodes, version 1.2, for this analysis (available at https://phewascatalog.org; ref. 71). The parent Phecode for asthma (Phecode 495) has 3 child concepts: (Phecode 495.1), chronic obstructive asthma; (Phecode 495.11), chronic obstructive asthma with exacerbation; and (Phecode 495.2), asthma with exacerbation. Each of these Phecodes represents a grouping of ICD-9 codes. Phecodes are hierarchical, and organized similarly to ICD codes. Thus, all cases for Phecode 495.1 are also cases for the parent code 495. A case is required to have 2 or more Phecodes on unique billing days. Noncases with ICDs for similar conditions are excluded from the analysis. Controls who had Phecodes in the range 490 to 498 were excluded. Association testing was conducted using Fisher's exact test. A Bonferroni's correction of 0.0125 was applied to account for the 4 tests conducted. The UK Biobank association test results were retrieved from Gene Atlas (http://geneatlas.roslin.ed.ac.uk/phewas/?variant=rs138619017&representation = table). The subtypes of asthma tested in the BioVU population were not available in the UK Biobank. The effect found in the much larger UK Biobank is within the confidence intervals of the association with asthma in BioVU (CI = 95% 0.9549–2.626).

Statistics

Data are represented as mean ± SEM. Comparisons between 2 groups were made using a 2-tailed Student's *t* test in Graphpad Prism 8. Comparisons between more than 2 groups were made using 1-way or 2-way ANOVA, where appropriate, followed by a Holm-Šidák post hoc test to correct for multiple comparisons in GraphPad Prism 8. Fisher's exact test followed by a per-SNP Bonferroni's correction was used to evaluate variant association. Data were considered significant at $P < 0.05$.

Study approval

All animal studies were approved by the IACUC at VUMC, and mice were bred and maintained using protocols approved by the IACUC at VUMC. Experiments were in compliance with ethical regulations for animal research. All human studies were approved by the IRB at VUMC, and subjects were recruited using protocols approved by VUMC's IRB. All participants provided written informed consent before enrollment.

Author contributions

AEN and RSP designed the studies. AEN, MHB, JZ, WZ, JYC, ZJC, ST, VDG, LMC, LMR, and NUC performed the experiments. AEN analyzed the data. DMA, DCN, TAC, and LB provided expertise and reviewed the manuscript. JW and LB performed bioinformatics analyses. KP and VVP performed blinded scoring of histological slides. TAC provided *Foxp3*^{EGFPcre}×*Rosa26*$^{YFP/YFP}$ mice. AEN and RSP wrote the manuscript.

Acknowledgments

The authors thank David Flaherty and Brittany Matlock of the VUMC Flow Cytometry Shared Resource for their assistance with sorting and use of the Aurora Cytek. The VUMC Flow Cytometry Shared Resource is supported by the Vanderbilt Ingram Cancer Center (P30 CA68485) and the Vanderbilt Digestive Disease Research Center (DK058404).

Address correspondence to: R. Stokes Peebles Jr., T-1218 MCN, Vanderbilt University Medical Center, 1161 21st Avenue South, Nashville, Tennessee 37232-2650, Phone: 615.322.3412; Email: stokes.peebles@vumc.org.

1. Sakaguchi S, et al. Regulatory T cells and immune tolerance. *Cell*. 2008;133(5):775–787.
2. Kim JM, et al. Regulatory T cells prevent catastrophic autoimmunity throughout the lifespan of mice. *Nat Immunol*. 2007;8(2):191–197.
3. Hori S, et al. Control of regulatory T cell development by the transcription factor Foxp3. *Science*. 2003;299(5609):1057–1061.
4. Wan YY, Flavell R. Regulatory T-cell functions are subverted and converted owing to attenuated Foxp3 expression. *Nature*. 2007;445(7129):766–770.
5. Bennett CL, et al. The immune dysregulation, polyendocrinopathy, enteropathy, X-linked syndrome (IPEX) is caused by mutations of FOXP3. *Nat Genet*. 2001;27(1):20–21.
6. Wildin RS, et al. X-linked neonatal diabetes mellitus, enteropathy and endocrinopathy syndrome is the human equivalent of mouse scurfy. *Nat Genet*. 2001;27(1):18–20.
7. Brunkow ME, et al. Disruption of a new forkhead/winged-helix protein, scurfin, results in the fatal lymphoproliferative disorder of the scurfy mouse. *Nat Genet*. 2001;27(1):68–73.
8. Marques CR, et al. Genetic and epigenetic studies of FOXP3 in asthma and allergy. *Asthma Res Pract*. 2015;1:10.
9. Shevach EM, Thornton AM. tTregs, pTregs, and iTregs: Similarities and differences. *Immunol Rev*. 2014;259(1):88–102.
10. Pawankar R, et al. Introduction and Executive Summary. In: Pawankar, et al, eds. *White Book on Allergy*. World Alergy Orginization. 2011:11–22.
11. Eder W, et al. The asthma epidemic. *N Engl J Med*. 2006;355(21):2226–2235.
12. Licona-Limon P, et al. TH2, allergy and group 2 innate lymphoid cells. *Nat Immunol*. 2013;14(6):536–42.
13. Palomares O, et al. Mechanisms of immune regulation in allergic diseases: the role of regulatory T and B cells. *Immunol Rev*. 2017;278(1):219–236.
14. Noval Rivas M, Chatila TA. Regulatory T cells in allergic diseases. *J Allergy Clin Immunol*. 2016;138(3):639–652.
15. Palm NW, et al. Allergic host defences. *Nature*. 2012;484(7395):465–72.
16. Wing JB, Sakaguchi S. Multiple treg suppressive modules and their adaptability. *Front Immunol*. 2012;3:178.
17. Wohlfert EA, et al. GATA3 controls Foxp3+ regulatory T cell fate during inflammation in mice. *J Clin Invest*. 2011;121(11):4503–4515.
18. Zheng Y, et al. Regulatory T-cell suppressor program co-opts transcription factor IRF4 to control TH2 responses. *Nature*. 2009;458(7236):351–356.
19. Chen CC, et al. IL-33 dysregulates regulatory T cells and impairs established immunologic

tolerance in the lungs. *J Allergy Clin Immunol*. 2017;140(5):1351–1363.
20. Harb H, et al. A regulatory T cell Notch4–GDF15 axis licenses tissue inflammation in asthma. *Nat Immunol*. 2020;21(11):1359–1370.
21. Ulges A, et al. Protein kinase CK2 enables regulatory T cells to suppress excessive TH2 responses in vivo. *Nat Immunol*. 2015;16(3):267–275.
22. Delacher M, et al. Rbpj expression in regulatory T cells is critical for restraining TH2 responses. *Nat Commun*. 2019;10(1):1621.
23. Suciu-Foca N, Cortesini R. Central role of ILT3 in the T suppressor cell cascade. *Cell Immunol*. 2007;248(1):59–67.
24. Zeldin DC. Epoxygenase pathways of arachidonic acid metabolism. *J Biol Chem*. 2001;276(39):36059–36062.
25. Dorris SL, Peebles RS. PGI2 as a regulator of inflammatory diseases. *Mediators Inflamm*. 2012;2012:926968.
26. Moncada S, et al. An enzyme isolated from arteries transforms prostaglandin endoperoxides to an unstable substance that inhibits platelet aggregation. *Nature*. 1976;263(5579):663–665.
27. Takahashi Y, et al. Augmentation of allergic inflammation in prostanoid IP receptor deficient mice. *Br J Pharmacol*. 2002;137(3):315–322.
28. Nagao K, et al. Role of prostaglandin I2 in airway remodeling induced by repeated allergen challenge in mice. *Am J Respir Cell Mol Biol*. 2003;29(3):314–320.
29. Jaffar Z, et al. Prostaglandin I2 -IP signaling blocks allergic pulmonary inflammation by preventing recruitment of $CD4^+$ Th2 cells into the airways in a mouse model of asthma. *J Immunol*. 2007;179(9):6193–6203.
30. Zhou W, et al. Prostaglandin I2 suppresses proinflammatory chemokine expression, CD4 T cell activation, and STAT6-independent allergic lung inflammation. *J Immunol*. 2016;197(5):1577–1586.
31. Zhou W, et al. The PGI2 analog cicaprost inhibits IL-33–induced Th2 responses, IL-2 production, and CD25 expression in mouse CD4 + T cells. *J Immunol*. 2018;201(7):1936–1945.
32. Zhou W, et al. Cyclooxygenase inhibition abrogates aeroallergen-induced immune tolerance by suppressing prostaglandin I2 receptor signaling. *J Allergy Clin Immunol*. 2014;134(3):698–705.
33. Zhou W, et al. Prostaglandin I2 analogs inhibit proinflammatory cytokine production and T cell stimulatory function of dendritic cells. *J Immunol*. 2007;178(2):702–710.
34. Zhou W, et al. Prostaglandin I2 analogs inhibit Th1 and Th2 effector cytokine production by CD4 T cells. *J Leukoc Biol*. 2007;81(3):809–817.
35. Li H, et al. Cyclooxygenase-2 regulates Th17 cell differentiation during allergic lung inflammation. *Am J Respir Crit Care Med*. 2011;184(1):37–49.
36. Massoud AH, et al. An asthma-associated IL4R variant exacerbates airway inflammation by promoting conversion of regulatory T cells to TH17-like cells. *Nat Med*. 2016;22(9):1013–1022.
37. Noval Rivas M, et al. Regulatory T cell reprogramming toward a Th2-cell-like lineage impairs oral tolerance and promotes food allergy. *Immunity*. 2015;42(3):512–523.
38. Li X, et al. Function of a Foxp3 cis-element in protecting regulatory T cell identity. *Cell*. 2014;158(4):734–748.
39. Williams LM, Rudensky AY. Maintenance of the Foxp3-dependent developmental program in mature regulatory T cells requires continued expression of Foxp3. *Nat Immunol*. 2007;8(3):277–284.
40. Williams JW, et al. Transcription factor IRF4 drives dendritic cells to promote Th2 differentiation. *Nat Commun*. 2013;4(1):2990.
41. Gao Y, et al. Control of T helper 2 responses by transcription factor IRF4-dependent dendritic cells. *Immunity*. 2013;39(4):722–732.
42. Harakal J, et al. Regulatory T cells control Th2-dominant murine autoimmune gastritis. *J Immunol*. 2016;197(1):27–41.
43. Liew FY, et al. Interleukin-33 in health and disease. *Nat Rev Immunol*. 2016;16(11):676–689.
44. Malek TR. The biology of IL-2. *Annu Rev Immunol*. 2008;26:453–479.
45. Chinen T, et al. An essential role for the IL-2 receptor in T reg cell function. *Nat Immunol*. 2016;17(11):1322–1333.
46. Chaudhary KR, et al. Efficacy of treprostinil in the SU5416-hypoxia model of severe pulmonary arterial hypertension: haemodynamic benefits are not associated with improvements in arterial remodelling. *Br J Pharmacol*. 2018;175(20):3976–3989.
47. Yang J, et al. Smad-dependent and smad-independent induction of id1 by prostacyclin analogues inhibits proliferation of pulmonary artery smooth muscle cells in vitro and in vivo. *Circ Res*. 2010;107(2):252–262.
48. Levarge BL. Prostanoid therapies in the management of pulmonary arterial hypertension. *Ther Clin Risk Manag*. 2015;11:535–547.
49. Zhou L, et al. Endothelial-like progenitor cells engineered to produce prostacyclin rescue monocrotaline-induced pulmonary arterial hypertension and provide right ventricle benefits. *Circulation*. 2013;128(9):982–994.
50. Hashimoto A, et al. Cilostazol induces PGI2 production via activation of the downstream epac-1/rap1 signaling cascade to increase intracellular calcium by PLCε and to activate p44/42 MAPK in human aortic endothelial cells. *PLoS One*. 2015;10(7):e0132835.
51. McKean JS, et al. The cAMP-producing agonist beraprost inhibits human vascular smooth muscle cell migration via exchange protein directly activated by cAMP. *Cardiovasc Res*. 2015;107(4):546–555.
52. Roden DM, et al. Development of a large-scale de-identified DNA biobank to enable personalized medicine. *Clin Pharmacol Ther*. 2008;84(3):362–369.
53. Stitham J, et al. Comprehensive biochemical analysis of rare prostacyclin receptor variants: study of association of signaling with coronary artery obstruction. *J Biol Chem*. 2011;286(9):7060–7069.
54. Canela-Xandri O, et al. An atlas of genetic associations in UK Biobank. *Nat Genet*. 2018;50(11):1593–1599.
55. Xiao J, et al. PD-1 upregulation is associated with exhaustion of regulatory T cells and reflects immune activation in HIV-1-infected individuals. *AIDS Res Hum Retroviruses*. 2019;35(5):444–452.
56. Yang K, et al. Homeostatic control of metabolic and functional fitness of T reg cells by LKB1 signalling. *Nature*. 2017;548(7669):602–606.
57. Wong CT, et al. Prostaglandin E2 alters Wnt-dependent migration and proliferation in neuroectodermal stem cells: Implications for autism spectrum disorders. *Cell Commun Signal*. 2014;12(1):1–18.
58. Harb J, et al. Recent development of Wnt signaling pathway inhibitors for cancer therapeutics. *Curr Oncol Rep*. 2019;21(2):12.
59. Gattinoni L, et al. Wnt/β-Catenin signaling in T-cell immunity and cancer immunotherapy. *Clin Cancer Res*. 2010;16(19):4695–4701.
60. Ma J, et al. β-catenin/TCF-1 pathway in T cell development and differentiation. *J Neuroimmune Pharmacol*. 2012;7(4):750–762.
61. Moffatt MF, et al. A large-scale, consortium-based genomewide association study of asthma. *N Engl J Med*. 2010;363(13):1211–1221.
62. Torgerson DG, et al. Meta-analysis of genome-wide association studies of asthma in ethnically diverse North American populations. *Nat Genet*. 2011;43(9):887–892.
63. Gudbjartsson DF, et al. Sequence variants affecting eosinophil numbers associate with asthma and myocardial infarction. *Nat Genet*. 2009;41(3):342–347.
64. Cho SA, et al. Analysis of genetic polymorphism and biochemical characterization of a functionally decreased variant in prostacyclin synthase gene (CYP8A1) in humans. *Arch Biochem Biophys*. 2015;569:10–18.
65. Idzko M, et al. Inhaled iloprost suppresses the cardinal features of asthma via inhibition of airway dendritic cell function. *J Clin Invest*. 2007;117(2):464–472.
66. Liu W, et al. Prostaglandin I2-IP signalling regulates human Th17 and Treg cell differentiation. *Prostaglandins Leukot Essent Fatty Acids*. 2013;89(5):335–344.
67. Tamosiuniene R, et al. A dominant role for regulatory T cells in protecting females against pulmonary hypertension. *Circ Res*. 2018;122(12):1689–1702.
68. Wong TH, et al. Dendritic cells treated with a prostaglandin I2 analog, iloprost, promote antigen-specific regulatory T cell differentiation in mice. *Int Immunopharmacol*. 2020;79:106106.
69. Castillo J, et al. CBP/p300 drives the differentiation of regulatory T cells through transcriptional and non-transcriptional mechanisms. *Cancer Res*. 2019;79(15):3916–3927.
70. Clapp LH, Gurung R. The mechanistic basis of prostacyclin and its stable analogues in pulmonary arterial hypertension: Role of membrane versus nuclear receptors. *Prostaglandins Other Lipid Mediat*. 2015;120:56–71.
71. Denny JC, et al. Systematic comparison of phenome-wide association study of electronic medical record data and genome-wide association study data. *Nat Biotechnol*. 2013;31(12):1102–1111.